Table of Contents

Supplementary Methods

Experimental Procedures

All melting points were determined on a micro melting point apparatus (RY-1G, Tianjin TianGuang Optical Instruments) and are uncorrected. Proton nuclear magnetic resonance (^{1}H-NMR) and carbon nuclear magnetic resonance (^{13}C-NMR) spectra were recorded in DMSO-d_6 on a Bruker AV-400 spectrometer with tetramethylsilane (TMS) as the internal standard. Coupling constants are given in hertz, and chemical shifts are reported in δ values (ppm) from TMS. All reactions were routinely monitored by thin layer chromatography (TLC) on Silica Gel GF254 for TLC, and spots were visualized with iodine vapor or by irradiation with UV light (λ = 254 nm). The mixture was brought to ambient temperature *via* air-jet cooling after completion of reaction. Flash column chromatography was performed on columns packed with Silica Gel (200-300 mesh), purchased from Qingdao Haiyang Chemical Company. Solvents were purified and dried by means of standard methods when necessary. Compounds purity were analyzed on a Shimadzu SPD-20A/20AV HPLC system with an Inertsil ODS-SP, 5 μm C18 column (150 mm × 4.6 mm). HPLC conditions: methanol/water with 0.1% formic acid 80:20; flow rate 1.0 mL/min; UV detection in 254 nm; temperature, ambient; injection volume, 20 μL. Purity of all tested compounds was above 95%.

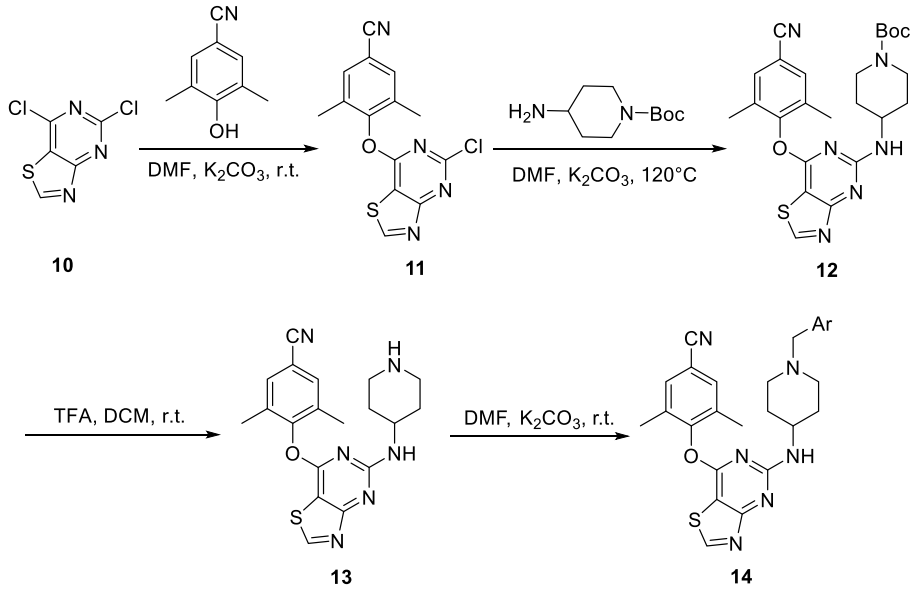

Supplementary Figure 1. Synthesis of **14a-f**

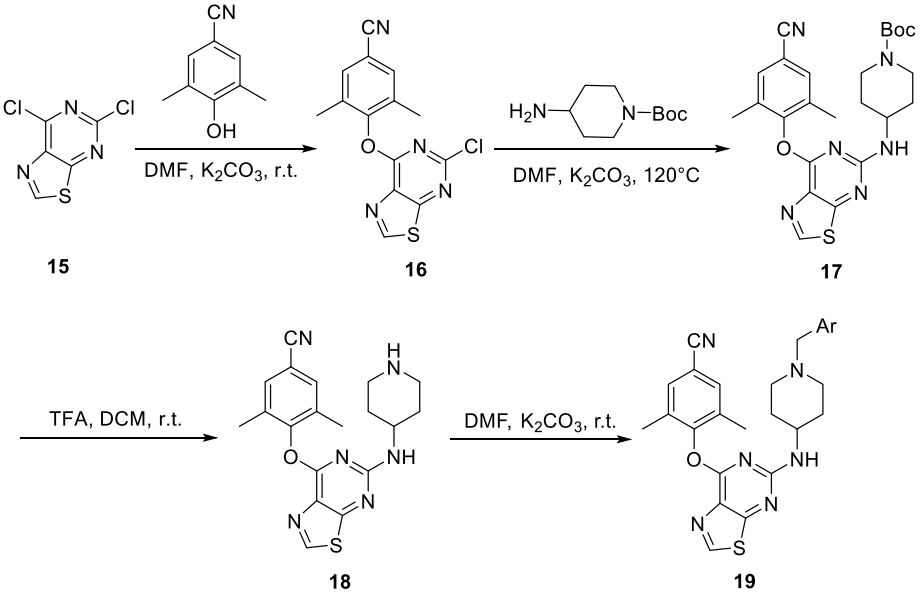

Supplementary Figure 2. Synthesis of **19a-f**

4-((2-chlorofuro[3,2-*d*]pyrimidin-4-yl)oxy)-3,5-dimethylbenzonitrile (6)

A reaction mixture of 4-hydroxy-3,5-dimethylbenzonitrile (**5**, 0.15 g, 1.0 mmol) and potassium carbonate (0.17 g, 1.2 mmol) in 3 mL of DMF was stirred at 25°C for 10 min, and then 2,4-dichlorofuro[3,2-*d*]pyrimidine (**11**, 0.18 g, 1.0 mmol) was added to it. Stirring was continued for an additional 1.5 h (monitored by TLC), then the mixture was poured into ice water, the precipitated white solid was collected by filtration, washed with cold water, and recrystallized in DMF-H_2O to provide the desired product **6** as white solid with 96% yield, mp: 225-228°C. ^{1}H NMR (400 MHz,

DMSO-d_6) δ 8.66 (d, J = 2.2 Hz, 1H, C_6-furopyrimidine-H), 7.78 (s, 2H, C_3,C_5-Ph-H), 7.32 (d, J = 2.2 Hz, 1H, C_7-furopyrimidine-H), 2.14 (s, 6H). HRMS: m/z 300.1111 [M + 1]$^+$. $C_{15}H_{10}ClN_3O_2$ (299.0462).

3,5-dimethyl-4-((2-(piperidin-4-ylamino)furo[3,2-*d*]pyrimidin-4-yl)oxy)benzonitrile (8).

A solution of **6** (0.30 g, 1.00 mmol), *tert*-butyl 4-aminopiperidine-1-carboxylate (0.24 g, 1.20 mmol), and anhydrous K_2CO_3 (0.27 g, 2.00 mmol) in 10 mL of DMF was heated at 120°C for 12 h. After completion (monitored by TLC), the mixture was cooled to room temperature and 50 mL of ice water was added. The reaction mixture was continuously stirred for another 30 min and the resulting precipitate was collected and dried to give the intermediate **7,** which was used directly without purification. To a solution of **7** (0.46 g, 1.00 mmol) in dichloromethane (DCM) (3 mL) was added trifluoroacetic acid (TFA) (1.10 mL, 15 mmol) at room temperature. After the mixture was stirred for 4 h (monitored by TLC), it was alkalized to pH 9 with saturated sodium bicarbonate solution and washed with saturated salt water (15 mL). The aqueous phase was extracted with DCM (3 × 5 mL). The combined organic phase was dried over Na_2SO_4. The filtrate was concentrated and purified by column chromatography on silica gel to get **8** as a white solid with 70% yield, mp: 123-125°C. ^{1}H NMR (400 MHz, DMSO-d_6) δ 8.23 (d, J = 2.1 Hz, 1H, C_6-furopyrimidine-H), 7.78 (d, J = 8.0 Hz, 2H, C_3,C_5-Ph-H), 6.87 (s, 1H, C_7-furopyrimidine-H), 6.77 (s, 1H, NH), 3.62 (s, 1H), 2.73 – 2.72 (m, 2H), 2.12 (s, 6H), 1.72-1.53 (m, 3H), 1.40 – 1.24 (m, 3H). HRMS: m/z364.1297 [M + 1]$^+$. $C_{20}H_{21}N_5O_2$ (363.1695).

4-((4-((4-(4-cyano-2,6-dimethylphenoxy)furo[3,2-*d*]pyrimidin-2-yl)amino)piperidin-1-yl)methyl)benzenesulfonamide (9a)

Recrystallized from Ethyl acetate/Petroleum ether as a white solid, 66% yield, mp: 206-208°C. ^{1}H NMR (400 MHz, DMSO-d_6) δ 8.23 (d, J = 2.1 Hz, 1H, C_6-furopyrimidine-H), 7.78 (d, J = 8.0 Hz, 2H, C_3,C_5-Ph'-H), 7.72 (s, 2H, C_3,C_5-Ph''-H), 7.47 (d, J = 8.0 Hz, 2H, C_2,C_6-Ph'-H), 7.33 (s, 2H, SO_2NH_2), 6.88 (s, 1H, C_7-furopyrimidine-H), 6.77 (s, 1H, NH), 3.62 (s, 1H), 3.48 (s, 2H, N-CH_2), 2.72

(s, 2H), 2.12 (s, 6H), 1.72-1.53 (m, 3H), 1.40 – 1.24 (m, 3H). ^{13}C NMR (100 Hz, DMSO-d_6) δ 158.9, 153.3, 152.7, 143.3, 143.1, 133.2, 132.9, 129.4, 126.0, 119.0, 109.0, 107.2, 62.0, 60.2, 52.7, 31.7, 16.3. HRMS: m/z 533.1966 $[M + 1]^+$. $C_{27}H_{28}N_6O_4S$ (532.1893).

4-((4-((4-(4-cyano-2,6-dimethylphenoxy)furo[3,2-*d*]pyrimidin-2-yl)amino)piperidin-1-yl)methyl)benzamide (9b)

Recrystallized from Ethyl acetate/Petroleum ether as a white solid, 45% yield, mp: 237-240°C. ^{1}H NMR (400 MHz, DMSO-d_6) δ 8.23 (d, J = 2.2 Hz, 1H, C_6-furopyrimidine-H), 7.94 (s, 2H, $CONH_2$), 7.83 (d, J = 8.0 Hz, 2H, C_3,C_5-Ph'-H), 7.72 (s, 2H, C_3,C_5-Ph''-H), 7.34 (d, J = 8.3 Hz, 2H, C_2,C_6-Ph'-H), 6.87 (s, 1H, C_7-furopyrimidine-H), 6.76 (s, 1H, NH), 3.62 (s, 1H), 3.48 (s, 2H, N-CH_2), 2.72 (s, 2H), 2.12 (s, 6H), 1.93 – 1.20 (m, 6H). ^{13}C NMR (100 Hz, DMSO-d_6) δ 168.2, 158.9, 153.3, 152.7, 142.5, 133.4, 133.2, 132.9, 128.8, 127.8, 119.0, 107.2, 62.2, 56.5, 52.7, 31.7, 19.0, 16.3. HRMS: m/z 497.2300 $[M + 1]^+$. $C_{28}H_{28}N_6O_3$ (496.2223).

3,5-dimethyl-4-((2-((1-(4-(methylsulfonyl)benzyl)piperidin-4-yl)amino)furo[3,2-*d*]pyrimidin-4-yl)oxy)benzonitrile (9c)

Recrystallized from Ethyl acetate/Petroleum ether as a white solid, 56% yield, mp: 173-175°C. ^{1}H NMR (400 MHz, DMSO-d_6) δ 8.23 (d, J = 2.2 Hz, 1H, C_6-furopyrimidine-H), 7.88 (d, J = 8.0 Hz, 2H, C_3,C_5-Ph'-H), 7.72 (s, 2H, C_3,C_5-Ph''-H), 7.55 (d, J = 8.0 Hz, 2H C_2,C_6-Ph'-H), 6.88 (s, 1H, C_7-furopyrimidine-H), 6.75 (s, 1H, NH), 3.62 (s, 1H), 3.52 (s, 2H, N-CH_2), 3.21 (s, 3H), 2.71 (s, 2H), 2.12 (s, 6H), 1.84 – 1.06 (m, 6H). ^{13}C NMR (100 MHz, DMSO-d_6) δ 158.9, 145.4, 139.8, 133.2, 132.9, 129.7 127.4, 109.0, 107.2, 61.9, 52.8, 44.0, 40.5, 31.7, 16.3. HRMS: m/z 532.2017 $[M + 1]^+$. $C_{28}H_{29}N_5O_4S$ (531.1940).

3,5-dimethyl-4-((2-((1-(pyridin-4-ylmethyl)piperidin-4-yl)amino)furo[3,2-*d*]pyrimidin-4-yl)oxy)benzonitrile (9d)

Recrystallized from Ethyl acetate/Petroleum ether as a white solid, 44% yield, mp: 115-117°C. ^{1}H NMR (400 MHz, DMSO-d_6) δ 8.57 – 8.44 (m, 2H), 8.23 (d, J = 2.2 Hz, 1H, C_6-furopyrimidine-H), 7.72 (s, 2H, C_3,C_5-Ph''-H), 7.39 – 7.18 (m, 2H),

6.88 (s, 1H, C_7-furopyrimidine-H), 6.79 (s, 1H, NH), 3.62 (s, 1H), 3.51 (s, 2H, N-CH_2), 2.72 (s, 2H), 2.12 (s, 6H), 1.89 – 1.70 (m, 3H), 1.52 – 1.31 (m, 3H). ^{13}C NMR (100 MHz, DMSO-d_6) δ 158.9, 153.3, 152.7, 149.9, 148.1, 133.2, 132.9, 124.1, 119.0, 109.0, 107.2, 61.2, 56.4, 52.8, 39.8, 31.6, 19.0, 16.3. HRMS: m/z 455.2194 [M + 1]$^+$. $C_{26}H_{26}N_6O_2$ (454.2117).

3,5-dimethyl-4-((2-((1-(4-nitrobenzyl)piperidin-4-yl)amino)furo[3,2-*d*]pyrimidin-4-yl)oxy)benzonitrile (9e)

Recrystallized from Ethyl acetate/Petroleum ether as a white solid, 45% yield, mp: 184-187°C. ^{1}H NMR (400 MHz, DMSO-d_6) δ 8.24 (d, *J* = 2.2 Hz, 1H, C_6-furopyrimidine-H), 8.19 (d, *J* = 8.6 Hz, 2H, C_3,C_5-Ph'-H), 7.72 (s, 2H, C_3,C_5-Ph''-H), 7.57 (d, *J* = 8.4 Hz, 2H, C_2,C_6-Ph'-H), 6.88 (s, 1H, C_7-furopyrimidine-H), 6.79 (s, 1H, NH), 3.56 (s, 2H), 2.72 (s, 2H), 2.12 (s, 6H), 1.85 – 1.69 (s, 3H), 1.52 – 1.21 (s, 3H). ^{13}C NMR (100 MHz, DMSO-d_6) δ 158.9, 153.3, 152.7, 147.5, 146.9, 133.2, 132.9, 130.0, 123.8, 119.0, 109.0, 107.2, 61.6, 56.4, 52.7, 31.7, 19.0, 16.3. HRMS: m/z 499.2090 [M + 1]$^+$. $C_{27}H_{26}N_6O_4$ (498.2016).

3-((4-((4-(4-cyano-2,6-dimethylphenoxy)furo[3,2-*d*]pyrimidin-2-yl)amino)piperidin-1-yl)methyl)benzamide (9f)

Recrystallized from Ethyl acetate/Petroleum ether as a white solid, 63% yield, mp: 193-195°C. ^{1}H NMR (400 MHz, DMSO-d_6) δ 8.23 (d, *J* = 2.2 Hz, 1H, C_6-furopyrimidine-H), 7.98 (s, 1H, C_2-Ph'-H), 7.81 – 7.74 (m, 2H), 7.72 (s, 2H, C_3,C_5-Ph''-H), 7.46 – 7.29 (m, 3H), 6.88 (s, 1H, C_7-furopyrimidine-H), 6.77 (s, 1H, NH), 3.61 (s, 2H), 2.73 (s, 2H), 2.12 (s, 6H), 1.89 – 1.61 (s, 3H), 1.47 – 1.25 (s, 3H). ^{13}C NMR (100 MHz, DMSO-d_6) δ 168.4, 158.9, 152.7, 139.2, 134.6, 133.2, 132.9, 132.0, 128.4, 126.4, 109.0, 107.3, 62.4, 56.5, 52.7, 31.7, 19.0, 16.3. HRMS: m/z 497.2299 [M + 1]$^+$. $C_{28}H_{28}N_6O_3$ (496.2223).

4-((5-chlorothiazolo[4,5-*d*]pyrimidin-7-yl)oxy)-3,5-dimethylbenzonitrile (11)

The synthetic method was similar to that described for **6**, except that the starting material 4-hydroxy-3,5-dimethylbenzonitrile (**5**, 0.15 g, 1.0 mmol) was reacted with 5,7-dichlorothiazolo[4,5-*d*]pyrimidine (0.20 g, 1.0 mmol). White solid, 94% yield, mp:

250-253°C. ^{1}H NMR (400 MHz, DMSO-d_6) δ 9.60 (s, 1H), 7.78 (s, 2H), 2.14 (s, 6H). HRMS: m/z 317.0255 $[M + 1]^+$. $C_{14}H_9ClN_4OS$ (316.0186).

3,5-dimethyl-4-((5-(piperidin-4-ylamino)thiazolo[4,5-d]pyrimidin-7-yl)oxy)benzonitrile (13)

The synthetic method was similar to that described for **8**. White solid, 64% yield, mp: 130-132°C. ^{1}H NMR (400 MHz, DMSO-d_6) δ 9.12 (s, 1H, thiazole-H), 8.50 (d, *J* = 5.9 Hz, 1H, NH), 7.67 (s, 2H, C_3,C_5-Ph-H), 3.65 – 3.62 (m, 1H), 2.78 – 2.76 (m, 2H), 2.10 (s, 6H), 1.86 – 1.75 (m, 2H), 1.72 – 1.55 (m, 4H). HRMS: m/z 381.1489 $[M + 1]^+$. $C_{19}H_{20}N_6OS$ (380.1419).

4-((4-((7-(4-cyano-2,6-dimethylphenoxy)thiazolo[4,5-*d*]pyrimidin-5-yl)amino)piperidin-1-yl)methyl)benzenesulfonamide (14a)

Recrystallized from Ethyl acetate/Petroleum ether as a white solid, 78% yield, mp: 139-142°C. ^{1}H NMR (400 MHz, DMSO-d_6) δ 9.06 (s, 1H, thiazole-H), 8.43 (d, *J* = 7.5 Hz, 1H, NH), 7.79 (d, *J* = 7.8 Hz, 2H, C_3,C_5-Ph'-H), 7.67 (s, 2H, C_3,C_5-Ph''-H), 7.47 (d, *J* = 8.0 Hz, 2H, C_2,C_6-Ph'-H), 7.32 (s, 2H, SO_2NH_2), 3.67 – 3.64 (m, 1H), 3.50 (s, 2H, N-CH_2), 2.81 – 2.67 (m, 2H), 2.09 (s, 6H), 1.88 – 1.75 (m, 2H), 1.65 – 1.39 (s, 4H). ^{13}C NMR (100 MHz, DMSO-d_6) δ 156.7, 154.5, 150.0, 143.3, 143.6, 132.9, 132.7, 129.0, 126.1, 119.3, 108.9, 61.9, 52.1, 48.4, 39.4, 31.5, 16.2. HRMS: m/z 550.1692 $[M + 1]^+$. $C_{26}H_{27}N_7O_3S_2$ (549.1617).

4-((4-((7-(4-cyano-2,6-dimethylphenoxy)thiazolo[4,5-*d*]pyrimidin-5-yl)amino)piperidin-1-yl)methyl)benzamide (14b)

Recrystallized from Ethyl acetate/Petroleum ether as a white solid, 51% yield, mp: 172-174°C. ^{1}H NMR (400 MHz, DMSO-d_6) δ 9.06 (s, 1H, thiazole-H), 8.43 (d, *J* = 7.5 Hz, 1H, NH), 7.80 (d, *J* = 7.8 Hz, 2H, C_3,C_5-Ph'-H), 7.67 (s, 2H, C_3,C_5-Ph''-H), 7.45 (d, *J* = 8.0 Hz, 2H, C_2,C_6-Ph'-H), 7.31 (s, 2H, $CONH_2$), 3.68 – 3.64 (m, 1H), 3.48 (s, 2H, N-CH_2), 2.80 – 2.77 (m, 2H), 2.10 (s, 6H), 1.92 – 1.78 (m, 2H), 1.70 – 1.59 (m, 4H). ^{13}C NMR (100 MHz, DMSO-d_6) δ 168.2, 161.0, 156.5, 154.7, 150.9, 142.2, 133.7, 133.1, 132.7, 129.0, 127.7, 119.2, 108.8, 62.2, 52.4, 48.9, 39.6, 39.3, 31.1, 16.2. HRMS: m/z 514.2020 $[M + 1]^+$. $C_{27}H_{27}N_7O_2S$ (513.1947).

3,5-dimethyl-4-((5-((1-(4-(methylsulfonyl)benzyl)piperidin-4-yl)amino)thiazolo[4,5-*d*]pyrimidin-7-yl)oxy)benzonitrile (14c)

Recrystallized from Ethyl acetate/Petroleum ether as a white solid, 76% yield, mp: 118-120°C. ^{1}H NMR (400 MHz, DMSO-d_6) δ 9.07 (s, 1H, thiazole-H), 8.44 (d, *J* = 7.5 Hz, 1H, NH), 7.88 (d, *J* = 8.1 Hz, 2H, C_3,C_5-Ph'-H), 7.67 (s, 2H, C_3,C_5-Ph''-H), 7.59 (d, *J* = 8.1 Hz, 2H, C_2,C_6-Ph'-H), 3.65 – 3.63 (m, 1H), 3.55 (s, 2H, N-CH_2), 3.22 (s, 3H, SO_2CH_3), 2.78 (d, *J* = 11.4 Hz, 2H), 2.10 (s, 6H), 1.99 – 1.83 (m, 3H), 1.77 – 1.60 (m, 3H). ^{13}C NMR (100 MHz, DMSO-d_6) δ 163.3, 160.3, 154.4, 150.2, 145.4, 145.3, 139.8, 139.8, 139.5, 133.0, 132.7, 129.8, 127.4, 119.0, 108.9, 108.2, 62.6 , 61.8, 52.7, 48.8, 44.1, 44.0, 39.4, 31.5, 31.1, 16.2. HRMS: m/z 549.1737 $[M + 1]^+$. $C_{27}H_{28}N_6O_3S_2$ (548.1664).

3,5-dimethyl-4-((5-((1-(pyridin-4-ylmethyl)piperidin-4-yl)amino)thiazolo[4,5-*d*]pyrimidin-7-yl)oxy)benzonitrile (14d)

Recrystallized from Ethyl acetate/Petroleum ether as a white solid, 52% yield, mp: 118-120°C. ^{1}H NMR (400 MHz, DMSO-d_6) δ 9.07 (s, 1H, thiazole-H), 8.52 (d, *J* = 5.9 Hz, 1H, NH), 8.46 (d, *J* = 7.5 Hz, 2H, C_3,C_5-Ph'-H), 7.67 (s, 2H, C_3,C_5-Ph''-H), 7.32 (d, *J* = 7.2 Hz, 2H, C_2,C_6-Ph'-H), 3.65 (dt, *J* = 8.2, 5.6 Hz, 1H), 3.48 (s, 2H, N-CH_2), 2.78 – 2.76 (m, 2H), 2.10 (s, 6H), 1.86 (dd, *J* = 11.8, 2.7 Hz, 2H), 1.72 – 1.55 (m, 4H). ^{13}C NMR (100 MHz, DMSO-d_6) δ 163.3, 161.1, 160.3, 156.5, 154.4, 150.2, 150.0, 149.9, 148.0, 133.0, 132.7, 128.2, 124.1, 119.0, 108.2, 61.2, 52.7, 48.7, 39.4, 31.1, 26.8, 16.2. HRMS: m/z 472.1917 $[M + 1]^+$. $C_{25}H_{25}N_7OS$ (471.1841).

3,5-dimethyl-4-((5-((1-(4-nitrobenzyl)piperidin-4-yl)amino)thiazolo[4,5-*d*]pyrimidin-7-yl)oxy)benzonitrile (14e)

Recrystallized from Ethyl acetate/Petroleum ether as a white solid, 66% yield, mp: 145-147°C. ^{1}H NMR (400 MHz, DMSO-d_6) δ 9.06 (s, 1H, thiazole-H), 8.45 (d, *J* = 7.6 Hz, 1H, NH), 8.21 (d, *J* = 8.4 Hz, 2H, C_3,C_5-Ph'-H), 7.67 (s, 2H, C_3,C_5-Ph''-H), 7.59 (d, *J* = 8.8 Hz, 2H, C_2,C_6-Ph'-H), 3.65 – 3.63 (m, 1H), 3.59 (s, 2H, N-CH_2), 2.78 (d, *J* = 11.5 Hz, 2H), 2.09 (s, 6H), 1.89 (dd, *J* = 12.7, 10.1 Hz, 2H), 1.78 – 1.50 (m, 4H). ^{13}C NMR (101 MHz, DMSO-d_6) δ 163.3, 161.2, 156.6, 154.4, 150.4, 147.0,

133.0, 132.7, 130.1, 130.0, 123.8, 61.6, 52.7, 48.7, 39.8, 39.6, 39.4, 31.1, 16.2. ESI-MS: m/z 516.1814 $[M + 1]^+$. $C_{26}H_{25}N_7O_3S$ (515.1740).

3-((4-((7-(4-cyano-2,6-dimethylphenoxy)thiazolo[4,5-*d*]pyrimidin-5-yl)amino)piperidin-1-yl)methyl)benzamide (14f)

Recrystallized from Ethyl acetate/Petroleum ether as a white solid, 74% yield, mp: 153-155°C. ^{1}H NMR (400 MHz, DMSO-d_6) δ 8.95 (s, 1H, thiazole-H), 7.97 (s, 1H, NH), 7.78 (d, J = 8.0 Hz, 2H, C_3,C_5-Ph'-H), 7.73 (s, 2H, C_3,C_5-Ph''-H), 7.45 (d, J = 8.4 Hz, 2H, C_2,C_6-Ph'-H), 7.37 (s, 2H, $CONH_2$), 3.71 (s, 1H), 3.48 (s, 2H, N-CH_2), 2.84 – 2.65 (m, 2H), 2.12 (s, 6H), 2.03 – 1.75 (m, 3H), 1.63 – 1.26 (m, 3H). ^{13}C NMR (100 MHz, DMSO-d_6) δ 168.4, 163.7, 161.1, 156.2, 154.4, 150.4, 139.9, 134.4, 133.0, 132.6, 132.1, 128.7, 128.2, 126.0, 119.2, 108.4, 62.4, 52.3, 48.8, 31.7, 16.2. HRMS: m/z 514.2022 $[M + 1]^+$. $C_{27}H_{27}N_7O_2S$ (513.1947).

4-((5-chlorothiazolo[5,4-*d*]pyrimidin-7-yl)oxy)-3,5-dimethylbenzonitrile (16)

The synthetic method was similar to that described for **6**, except that the starting material 4-hydroxy-3,5-dimethylbenzonitrile (**5**, 0.15 g, 1.0 mmol) was reacted with 5,7-dichlorothiazolo[5,4-*d*]pyrimidine (0.20 g, 1.0 mmol). White solid, 93% yield, mp: 265-268°C. ^{1}H NMR (400 MHz, DMSO-d_6) δ 9.06 (s, 1H), 7.67 (s, 2H, C_3,C_5-Ph-H), 2.14 (s, 6H). ESI-MS: m/z 317.0260 $[M + 1]^+$. $C_{14}H_9ClN_4OS$ (316.0186).

3,5-dimethyl-4-((5-(piperidin-4-ylamino)thiazolo[4,5-*d*]pyrimidin-7-yl)oxy)b enzonitrile (18)

The synthetic method was similar to that described for **8**. White solid, 90% yield, mp: 135-138°C. ^{1}H NMR (400 MHz, DMSO-d_6) δ 9.06 (s, 1H, thiazole-H), 8.42 (d, J = 7.2 Hz, 1H, NH), 7.67 (s, 2H, C_3,C_5-Ph-H), 3.65– 3.63 (m, 1H), 2.79 – 2.78 (m, 2H), 2.10 (s, 6H), 1.86 – 1.82 (m, 2H), 1.70 – 1.52 (m, 4H). HRMS: m/z 381.1492 $[M + 1]^+$. $C_{19}H_{20}N_6OS$ (380.1419).

4-((4-((7-(4-cyano-2,6-dimethylphenoxy)thiazolo[5,4-*d*]pyrimidin-5-yl)amino)piperidin-1-yl)methyl)benzenesulfonamide (19a)

Recrystallized from Ethyl acetate/Petroleum ether as a white solid, 66% yield, mp: 158-161°C. ^{1}H NMR (400 MHz, DMSO-d_6) δ 9.06 (s, 1H, thiazole-H), 8.44 (d, J

= 7.5 Hz, 1H, NH), 7.80 (d, *J* = 8.0 Hz, 2H, C_3,C_5-Ph'-H), 7.67 (s, 2H, C_3,C_5-Ph''-H), 7.49 (d, *J* = 8.3 Hz, 2H, C_2,C_6-Ph'-H), 7.33 (s, 2H, SO_2NH_2), 3.65 – 3.62 (m, 1H), 3.50 (s, 2H, N-CH_2), 2.78 – 2.76 (m, 2H), 2.09 (s, 6H), 1.88 – 1.83 (m, 3H), 1.71 – 1.62 (m, 3H). ^{13}C NMR (100 MHz, DMSO-d_6) δ 163.4, 161.2, 156.5, 154.5, 150.2, 143.2, 143.2, 133.0, 132.7, 129.5, 128.2, 126.1, 119.2, 108.2, 61.9, 52.7, 48.8, 31.1, 16.2. HRMS: m/z 550.1691 $[M + 1]^+$. $C_{26}H_{27}N_7O_3S_2$ (549.1617).

4-((4-((7-(4-cyano-2,6-dimethylphenoxy)thiazolo[5,4-*d*]pyrimidin-5-yl)amino)piperidin-1-yl)methyl)benzamide (19b)

Recrystallized from Ethyl acetate/Petroleum ether as a white solid, 51% yield, mp: 144-146°C. ^{1}H NMR (400 MHz, DMSO-d_6) δ 9.06 (s, 1H, thiazole-H), 8.43 (d, *J* = 7.5 Hz, 1H, NH), 7.84 (d, *J* = 7.9 Hz, 2H, C_3,C_5-Ph'-H), 7.67 (s, 2H, C_3,C_5-Ph''-H), 7.37 (d, *J* = 8.1 Hz, 2H, C_2,C_6-Ph'-H), 7.33 (s, 2H, $CONH_2$), 3.66 – 3.61 (m, 1H), 3.48 (s, 2H, N-CH_2), 2.79 – 2.76 (m, 2H), 2.10 (s, 6H), 1.86 – 1.81 (m, 2H), 1.70 – 1.60 (m, 4H). ^{13}C NMR (100 MHz, DMSO-d_6) δ 168.2, 163.3, 161.1, 156.5, 154.5, 150.2, 142.4, 133.4, 133.0, 132.7, 128.9, 128.2, 127.9, 119.2, 108.2, 62.2, 52.7, 48.9, 39.6, 39.4, 31.1, 16.2. HRMS: m/z 514.2019 $[M + 1]^+$. $C_{27}H_{27}N_7O_2S$ (513.1947).

3,5-dimethyl-4-((5-((1-(4-(methylsulfonyl)benzyl)piperidin-4-yl)amino)thiazolo[5,4-*d*]pyrimidin-7-yl)oxy)benzonitrile (19c)

Recrystallized from Ethyl acetate/Petroleum ether as a white solid, 59% yield, mp: 112-114°C. ^{1}H NMR (400 MHz, DMSO-d_6) δ 9.06 (s, 1H, thiazole-H), 8.44 (d, *J* = 7.5 Hz, 1H, NH), 7.90 (d, *J* = 8.0 Hz, 2H, C_3,C_5-Ph'-H), 7.67 (s, 2H, C_3,C_5-Ph''-H), 7.58 (d, *J* = 8.0 Hz, 2H, C_2,C_6-Ph'-H), 3.63 – 3.62 (m, 1H), 3.55 (s, 2H, N-CH_2), 3.22 (s, 3H, SO_2CH_3), 2.78 (d, *J* = 11.3 Hz, 2H), 2.10 (s, 6H), 1.98 – 1.81 (m, 2H), 1.77 – 1.51 (m, 4H). ^{13}C NMR (100 MHz, DMSO-d_6) δ 163.3, 161.1, 156.5, 154.4, 150.2, 145.3, 139.8, 133.0, 132.7, 129.8, 127.4, 127.2, 119.2, 108.2, 61.8, 52.7, 48.8, 44.0, 39.8, 39.4, 31.1, 16.2. HRMS: m/z 549.1714 $[M + 1]^+$. $C_{27}H_{28}N_6O_3S_2$ (548.1664).

3,5-dimethyl-4-((5-((1-(pyridin-4-ylmethyl)piperidin-4-yl)amino)thiazolo[5,4-*d*]pyrimidin-7-yl)oxy)benzonitrile (19d)

Recrystallized from Ethyl acetate/Petroleum ether as a white solid, 44% yield, mp: 116-118°C. ^{1}H NMR (400 MHz, DMSO-d_6) δ 9.07 (s, 1H, thiazole-H), 8.52 (d, *J* = 5.5 Hz, 1H, NH), 8.44 (d, *J* = 7.5 Hz, 2H, C_3,C_5-Ph'-H), 7.67 (s, 2H, C_3,C_5-Ph''-H), 7.34 – 7.29 (m, 2H, C_2,C_6-Ph'-H), 3.66 – 3.63 (m, 1H), 3.48 (s, 2H, N-CH_2), 2.78 – 2.76 (m, 2H), 2.10 (s, 6H), 1.90 – 1.84 (m, 3H), 1.74 – 1.36 (m, 3H). ^{13}C NMR (100 MHz, DMSO-d_6) δ 163.3, 156.6, 154.4, 150.2, 150.0, 149.9, 148.0, 133.0, 132.7, 128.2, 124.1, 119.2, 108.2, 61.2, 52.7, 48.7, 39.6, 31.1, 16.2. HRMS: m/z 472.1918 $[M + 1]^+$. $C_{25}H_{25}N_7OS$ (471.1841).

3,5-dimethyl-4-((5-((1-(4-nitrobenzyl)piperidin-4-yl)amino)thiazolo[5,4-*d*]pyrimidin-7-yl)oxy)benzonitrile (19e)

Recrystallized from Ethyl acetate/Petroleum ether as a white solid, 51% yield, mp: 146-148°C. ^{1}H NMR (400 MHz, DMSO-d_6) δ 9.07 (s, 1H, thiazole-H), 8.45 (d, *J* = 7.5 Hz, 1H, NH), 8.22 (d, *J* = 8.4 Hz, 2H, C_3,C_5-Ph'-H), 7.67 (s, 2H, C_3,C_5-Ph''-H), 7.59 (d, *J* = 8.5 Hz, 2H, C_2,C_6-Ph'-H), 3.65 (dt, *J* = 8.0, 5.2 Hz, 1H), 3.59 (s, 2H, N-CH_2), 2.78 (d, *J* = 11.3 Hz, 2H), 2.10 (s, 6H), 1.89 (dt, *J* = 11.6, 6.0 Hz, 2H), 1.78 – 1.55 (m, 4H). ^{13}C NMR (100 MHz, DMSO-d_6) δ 163.3, 161.1, 156.6, 154.4, 150.3, 147.4, 147.0, 133.0, 132.7, 130.1, 128.2, 123.8, 119.2, 108.2, 61.6, 52.7, 48.7, 31.1, 16.2. HRMS: m/z 516.1817 $[M + 1]^+$. $C_{26}H_{25}N_7O_3S$ (515.1740).

3-((4-((7-(4-cyano-2,6-dimethylphenoxy)thiazolo[5,4-*d*]pyrimidin-5-yl)amino)piperidin-1-yl)methyl)benzamide (19f)

Recrystallized from Ethyl acetate/Petroleum ether as a white solid, 73% yield, mp: 154-156°C. ^{1}H NMR (400 MHz, DMSO-d_6) δ 9.06 (s, 1H, thiazole-H), 8.44 (d, *J* = 7.6 Hz, 1H, NH), 7.80 (d, *J* = 8.4 Hz, 2H, C_3,C_5-Ph'-H), 7.67 (s, 2H, C_3,C_5-Ph''-H), 7.47 – 7.40 (m, 2H, C_2,C_6-Ph'-H), 7.37 (s, 2H, $CONH_2$), 3.76 – 3.57 (m, 1H), 3.48 (s, 2H, N-CH_2), 2.79 – 2.77 (m, 2H), 2.10 (s, 6H), 1.90 – 1.86 (m, 2H), 1.75 – 1.53 (m, 4H). ^{13}C NMR (100 MHz, DMSO-d_6) δ 168.4, 163.3, 161.1, 156.6, 154.4, 150.1, 139.1, 134.7, 133.0, 132.7, 132.1, 128.5, 128.2, 126.5, 119.2, 108.2, 62.4, 52.7, 48.8, 31.1, 16.2. HRMS: m/z 514.2020 $[M + 1]^+$. $C_{27}H_{27}N_7O_2S$ (513.1947).

In vitro assay of anti-HIV activities in MT-4 cells

The anti-HIV activity and cytotoxicity of the newly synthesized derivatives were evaluated with WT HIV-1 (HIV-IIIB strain), single RT mutant strains (L100I, K103N, Y181C, Y188L, and E138K), double RT mutant strains (F227L+V106A and K103N +Y181C), and HIV-2 (strain ROD) in MT-4 cell cultures using the 3-(4,5-dimethylthiazol-2-yl)-2,5-diphenyltetrazolium bromide (MTT) method as described previously.[1, 2] At the beginning of each experiment, stock solutions (10×final concentration) of test compounds were added in 25 μL volumes to two series of triplicate wells in order to allow simultaneous evaluation of the effects on mock- and HIV-infected cells. Using a Biomek 3000 robot (Beckman Instruments, Fullerton, CA), serial five-fold dilutions of the test compounds (final 200 μL volume per well) were made directly in flat-bottomed 96-well microtiter trays, including untreated control HIV-1 and mock-infected cell samples for each sample. HIV-1 (IIIB) and mutant HIV-1 strains (K103N+Y181C, F227L+V106A, L100I, K103N, Y181C, Y188L and E138K) or HIV-2 (ROD) stock (50 μL at 100-300 $CCID_{50}$) (50% cell culture infectious dose) or culture medium was added to either the infected or mock-infected wells of the microtiter tray. Mock-infected cells were used to evaluate the effect of test compounds on uninfected cells in order to assess cytotoxicity. Exponentially growing MT-4 cells were centrifuged for 5 min at 1000 rpm and the supernatant was discarded. The MT-4 cells were resuspended at 6×105 cells/mL, and 50 μL aliquots were transferred to the microtiter tray wells. At five days after infection, the viability of mock- and HIV-infected cells was determined spectrophotometrically by means of MTT assay.

The MTT assay is based on the reduction of yellow-colored MTT (Acros Organics, Geel, Belgium) by mitochondrial dehydrogenase of metabolically active cells to form a blue-purple formazan that can be measured spectrophotometrically. The absorbances were read in an eight-channel computer-controlled photometer (Multiscan Ascent Reader, Labsystems, Helsinki, Finland), at the wavelengths of 540 and 690 nm. All data were calculated using the median optical density (OD) value of three wells. The EC_{50} was defined as the concentration of the test compound affording 50% protection from viral cytopathogenicity. The CC_{50} was defined as the compound

concentration that reduced the absorbance (OD540) of mock-infected cells by 50%.

Supplementary Table 1. SI and RF values of the preferred compounds

Compds	SI (RF)[a]					
	L100I	**K103N**	**Y181C**	**Y188L**	**E138K**	**F227L+V106A**
14a	3183 (2.6)	6367 (1.3)	3700 (2.2)	2173 (3.8)	3802 (2.2)	1323 (6.3)
14c	2938 (1.6)	2519 (1.9)	1374 (3.4)	896 (5.2)	1579 (3.0)	622 (7.6)
14d	5319 (3.3)	15661 (1.1)	5125 (3.4)	3862 (4.6)	5421 (3.3)	906 (19.4)
19a	2382 (3.6)	12025 (0.7)	3507 (2.4)	2122 (4.0)	2903 (2.9)	1435 (6.0)
19b	4185 (3.8)	16001 (1.0)	5133 (3.1)	3676 (4.4)	5037 (3.2)	1302 (12.3)
19c	2280 (2.3)	3820 (1.4)	1703 (3.1)	1812 (2.9)	1936 (2.7)	846 (6.1)
19d	2091 (5.1)	8494 (1.3)	4942 (2.2)	4314 (2.5)	4384 (2.4)	931 (11.5)
ETV	>755 (1.1)	>1379 (0.6)	>315 (2.3)	>225 (3.3)	>471 (1.6)	>233 (3.2)

[a] RF is the ratio of $EC_{50(\text{resistant viral strain})}/EC_{50(\text{wild-type viral strain})}$.

Recombinant HIV-1 reverse transcriptase (RT) inhibitory assays

The HIV-1 RT inhibition assay was performed by using an RT assay kit produced by Roche. The procedure for assaying HIV-1 RT inhibition was conducted as described in the kit protocol.[2]

The reaction mixture containing HIV-1 RT enzyme, reconstituted template and viral nucleotides [digoxigenin (DIG)-dUTP, biotin-dUTP and dTTP] in the incubation buffer with or without inhibitors was incubated for 1 h at 37ºC firstly. Then, the mixture was transferred to a streptavidin-coated microtitre plate (MTP) and incubated for another 1 h at 37ºC. The biotin-labeled dNTPs that were incorporated into the cDNA chain in the presence of RT were bound to streptavidin. The unbound dNTPs were washed with washing buffer, and anti-DIG-POD was added to the MTPs.

After incubation for 1 h at 37ºC, the DIG-labeled dNTPs incorporated in cDNA were bound to the anti-DIG-POD antibody. The unbound anti-DIG-PODs were washed out and the peroxide substrate (ABTS) solution was added to the MTPs. The absorbance of the sample was determined at OD_{405} nm using a microtiter plate ELISA reader. The IC_{50} values correspond to the concentrations of the inhibitors required to

inhibit biotin-dUTP incorporation by 50%.

Molecular Modeling

Preparation of HIV-1 RT structures and ligand. The atomic coordinates for molecular modeling study were obtained from our recently published X-ray crystal structure (PDB ID: 6C0J, resolution: 1.92 Å) of HIV-1 RT and co-crystallized with **K-5a2**, which shares similar structural scaffold as compounds **14a**, **19a** and **19c**.[3] Protein structure was imported into the Maestro Module available in the Schrödinger Suite (Schrödinger, LLC) and structure was optimized as previously described.[4] Ligands 3D structures were built using the Maestro and preprocessed using the LigPrep module (v2.5) of the Schrödinger modeling software. Preprocessing includes energy minimization using the OPLS_2005 force field and determination of ionization states at pH = 7 (±2).[5]

Molecular docking and MM-GBSA calculations. To better understand the binding affinity difference of compounds **14a, 19a** and **19c** in various HIV-1 RT mutants (single mutants: L100I, K103N, Y181C, Y188L, E138K; and double mutants: F227L+V106A and Y181C+K103N) molecular docking followed by MM-GBSA calculations were performed as previously described.[6] The receptor grid generation and docking studies were performed using the Glide module available in the Schrödinger Suite. From docking, the best 25 poses for each mutation structure were selected for further MM-GBSA calculation. During binding affinity calculation, the program offers the option to treat the ligand and protein as flexible; in this study, a 5Å region of the protein around the ligand was treated as flexible. The poses with the highest binding affinity score ($\Delta G_{MMGBSA\text{-}bind}$) was chosen for further binding mode comparison in wild types and various mutant HIV-1 strains (**Table S2**). The theoretical background and procedures of Prime-MMGBSA as it is implemented in the Schrödinger are described in detail elsewhere.[7, 8, 9]

Supplementary Table 2. Summary of Prime-MMGBSA-based binding energies (in kcal/mol) of compound **19a** in various HIV-1 strains

HIV-1 strains	pIC_{50}	Docking score	ΔG_{Bind}	ΔG_{Bind} Coul	ΔG_{Bind} Covalent	ΔG_{Bind} vdW	ΔG_{Bind} HB	ΔG_{Bind} Lipo	ΔG_{Bind} Packing	ΔG_{Bind} Solv GB
WT	8.80	-13.52	-107.63	-27.44	2.03	-78.98	-2.19	-36.61	-4.74	40.29
L100I	8.02	-10.20	-76.94	-3.01	3.74	-74.49	0.25	-35.11	-3.40	35.07
K103N	8.72	-12.79	-106.96	-3.16	1.87	-75.20	-0.74	-40.81	-6.29	17.36
Y181C	8.19	-11.60	-88.23	-23.25	5.63	-67.39	-1.59	-34.54	-2.96	35.88
Y188L	7.97	-9.87	-79.54	-14.65	8.46	-72.92	-1.39	-31.82	-0.52	33.31
E138K	8.10	-10.97	-86.83	-12.73	6.51	-69.08	-1.23	-37.89	-4.25	31.83
F227L+V106A	7.80	-9.97	-76.18	-13.81	6.56	-69.96	-0.86	-32.49	-4.01	38.38
Y181C+K103N	7.74	-9.94	-72.30	-2.80	11.18	-73.77	-1.17	-35.29	-3.33	32.88

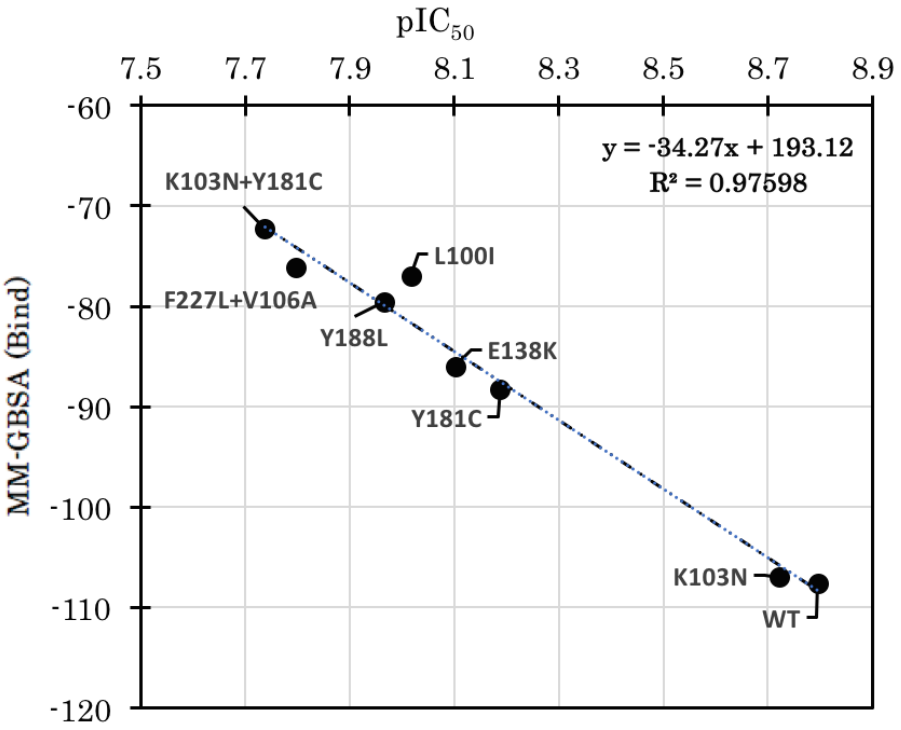

Supplementary Figure 3. Relationship between the observed inhibition (logarithmic unit) and the MM-GBSA relative affinity

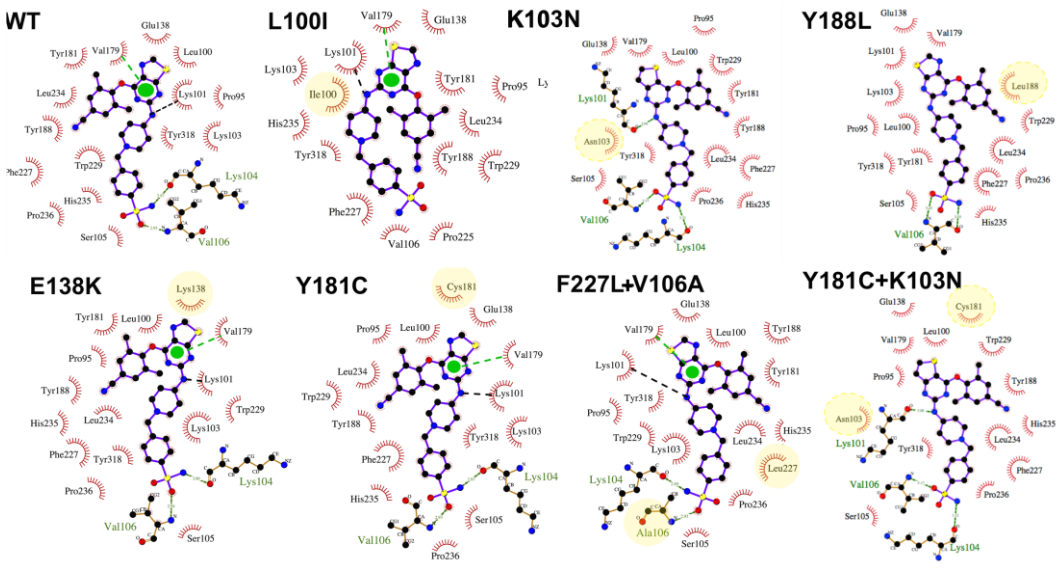

Supplementary Figure 4. Schematic 2D-representation of proten-ligand interaction of **19a** with various mutants is shown and key mutants are highlighted with yellow circle.

Cytochrome P450 inhibition assay

CYP1A2 Inhibition: Each compound in eight concentrations (0, 0.05, 0.15, 0.5, 1.5, 5.0, 15, 50 μM) is incubated with human liver microsomes (0.25 mg/mL) and NADPH (10 mM) in the presence of CYP1A2 probe substrate Phenacetin (100 μM) for 10 min at 37°C water bath. The selective CYP1A2 inhibitor, alpha-naphthoflavone (0, 0.0142, 0.0123, 0.037, 0.11, 0.33, 1.0, 3.0 μM), will be screened alongside the test compound as a positive control. Methanol containing tolbutamide as internal standard will be used for stopping reaction. Including positive controls, duplicates of **14a, 19a** and **19c** each concentration prepared in parallel.

CYP2C9 Inhibition: Each compound in eight concentrations (0, 0.05, 0.15, 0.5, 1.5, 5.0, 15, 50 μM) is incubated with human liver microsomes (0.25 mg/mL) and NADPH (10 mM) in the presence of CYP2C9 probe substrate Diclofenac (50 μM) for 10 min at 37°C water bath. The selective CYP2C9 inhibitor, Sulfaphenazole (0, 0.0142, 0.0123, 0.037, 0.11, 0.33, 1.0, 3.0 μM), will be screened alongside the test compound as a positive control. Methanol containing tolbutamide as internal standard will be used for stopping reaction. Including positive controls, duplicates of **14a, 19a** and **19c** each concentration prepared in parallel.

CYP2C19 Inhibition: Each compound in eight concentrations (0, 0.05, 0.15, 0.5, 1.5, 5.0, 15, 50 μM) is incubated with human liver microsomes (0.25 mg/mL) and NADPH (10 mM) in the presence of CYP2C19 probe substrate S-mephenytoin (300 μM) for 10 min at 37°C water bath. The selective CYP2C19 inhibitor, (+)-*N*-3-benzylnirvanol (0, 0.0142, 0.0123, 0.037, 0.11, 0.33, 1.0, 3.0 μM) will be screened alongside the test compound as a positive control. Methanol containing tolbutamide as internal standard will be used for stopping reaction. Including positive controls, duplicates of **14a, 19a** and **19c** each concentration prepared in parallel.

CYP2D6 Inhibition: Each compound in eight concentrations (0, 0.05, 0.15, 0.5, 1.5, 5.0, 15, 50 μM) is incubated with human liver microsomes (0.25 mg/mL) and NADPH (10 mM) in the presence of CYP2D6 probe substrate Dextromethorphan (50 μM) for 10 min at 37°C water bath. The selective CYP2D6 inhibitor, Quinidine (0,

0.0142, 0.0123, 0.037, 0.11, 0.33, 1.0, 3.0 μM) will be screened alongside the test compound as a positive control. Methanol containing tolbutamide as internal standard will be used for stopping reaction. Including positive controls, duplicates of **14a, 19a** and **19c** each concentration prepared in parallel.

CYP3A4M Inhibition: Each compound in eight concentrations (0, 0.05, 0.15, 0.5, 1.5, 5.0, 15, 50 μM) is incubated with human liver microsomes (0.25 mg/mL) and NADPH (10 mM) in the presence of CYP3A4M probe substrate Midazolam (20 μM) for 10 min at 37°C water bath. The selective CYP3A4M inhibitor, Ketoconazole (0, 0.0142, 0.0123, 0.037, 0.11, 0.33, 1.0, 3.0 μM) will be screened alongside the test compound as a positive control. Methanol containing tolbutamide as internal standard will be used for stopping reaction. Including positive controls, duplicates of **14a, 19a** and **19c** each concentration prepared in parallel.

Pharmacokinetics assays

Ten male Wistar rats (200-220 g) were randomly divided into two groups to receive oral administration (20 $mg.kg^{-1}$) or intravenous (2 $mg.kg^{-1}$). A solution of **14a** and **19a** was prepared by dissolving in a mixture of polyethylene glycol (peg) 400/normal saline (70/30, V/V). Blood samples of the intravenous group were collected from the sinus jugular is into heparinized centrifugation tubes at 2 min, 5 min, 15 min, 30 min, 1 h, 1.5 h, 2 h, 4 h and 8 h after dosing, and blood samples of the oral administration group were collected at 5 min, 15 min, 30 min, 1 h, 2 h, 4 h, 6 h, 8h, 12 h, and 24 h after dosing (200 μL of blood each times). All the samples were then centrifuged at 8000 rpm for 8 min to separate plasma, which was stored at -78°C until analysis. LC-MS/MS analysis was used to determine the concentration of **14a** and **19a** in plasma. Briefly, 50 μL of plasma was added to 50 μL of internal standard and 300 μL of methanol in a 5 mL centrifugation tube, which was centrifuged at 3000g for 10 min. The supernatant layer was collected and a 20 μL aliquot was injected for LC-MS/MS analysis. Standard curves for **14a** and **19a** in blood were generated by the addition of various concentrations of **14a** and **19a** together with internal standard to blank plasma. Then all samples were quantified with an Agilent 1200 LC/MSD (Agilent, USA). The mobile phase was methanol/1.5% glacial acetic

acid (50:50, V/V) at a flow rate of 1.0 mL/min, the test wavelength was 225 nm.

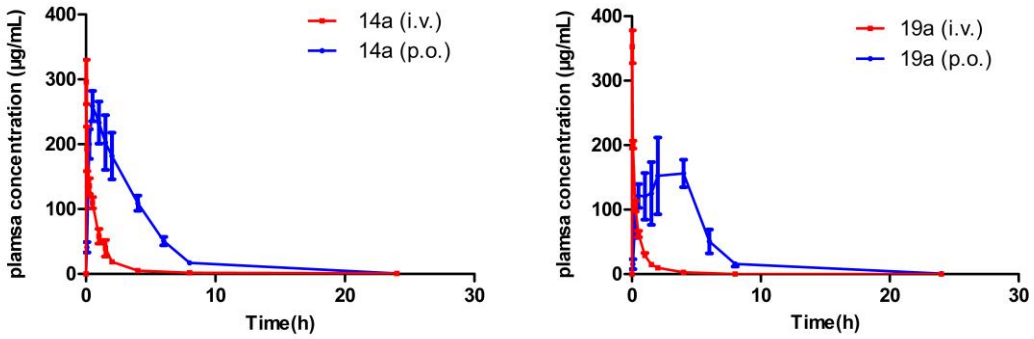

Supplementary Figure 5. Pharmacokinetics. The plasma concentration–time profiles of **14a** and **19a** in Wistar rats following oral administration (20 mg.kg^{-1}) and intravenous administration (2 mg.kg^{-1}). Data points represent ±SD

Acute toxicity experiment

Kunming mice (18-20 g) were purchased from the animal experimental center of Shandong University. Compounds **14a** and **19a** was suspended in PEG-400 and normal saline at concentrations of 100 mg•mL^{-1}, and administered intragastrically by gavage after the mice had been fasted for 12 hours. Dosage of 2000 mg•kg^{-1} was administered to 10 mice per group (5 males, 5 females). The death was monitored in-life observations.

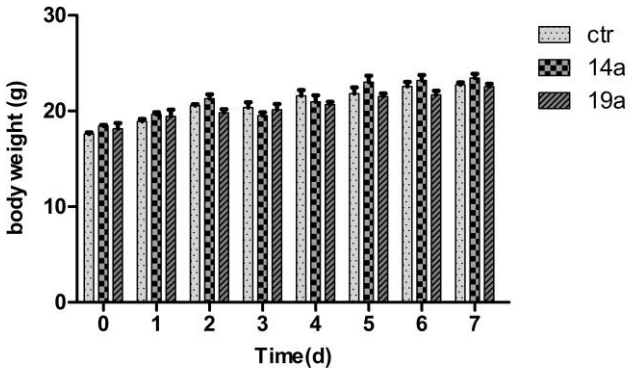

Supplementary Figure 6. The result of acute toxicity. The relative body weight changes of mice in different groups (control, **14a** and **19a**). Data points represent ±SD

Assay procedures for hERG activity[10]

HEK293 cells with stably transfected with hERG cDNA was selected to test the inhibitory activity to the hERG potassium channel. HEK239 cells expressing hERG

were plated in 35 mm dishes for 24 hours and maintained at 37 °C under 5% CO_2. A micropipette was drawn out from borosilicate glass to give a tip resistance between 3 ~ 5 MΩ. For each trial, a single dish of cells was removed from the incubator, washed two times with ECS and placed on the microscope stage. The whole-cell recordings were conducted with a commercial available patch clamp amplifier.

Tail currents were evoked once every 30 s by a 3 s, -50 mV repolarizing pulse following a 2 s, +50 mV depolarizing pulse with a hold voltage of -80 mV. A 50 ms depolarizing pulse to -50 mV at the beginning of the voltage protocol served as a baseline for calculating the amplitude of the peak tail current. Only stable cells with recording parameters exceed threshold were used for experiments. The hERG currents were allowed to stabilize over a 3-minute period under the condition that vehicle alone prior to test compound application. The cells were kept in the test solution until the peak tail current was stable (< 5% change) for ~5 sweeps. Peak tail amplitudes were then plotted as a function of the sweep number. Five peak tail current measurements at the steady state before the test compound application were averaged and used as the control current amplitude. Four or five peak tail current measurements at the steady state after test compound application were averaged and used as the remaining current amplitude after inhibition by the test compound.

Supplementary Table 3. Inhibitory effect of **14a** on hERG

Concentration (M)	**Inhibitory effect (%)**							**Mean±SD (%)**
	cell 1	**cell 2**	**cell 3**	**cell 4**	**cell 5**	**cell 6**	**cell 7**	
1.00×10^{-9}	NA	NA	NA	NA	-1.57	-2.48	-4.90	-2.98 ±1.72
3.00×10^{-9}	NA	NA	NA	NA	2.52	-3.51	-3.67	-1.56 ±3.53
3.00×10^{-7}	55.16	66.92	NA	68.74	NA	NA	NA	63.60 ±7.37
1.00×10^{-6}	72.67	83.59	NA	82.19	NA	NA	NA	79.49 ±5.94
3.00×10^{-6}	80.47	84.35	NA	88.55	NA	NA	NA	84.46 ±4.04
1.00×10^{-5}	81.94	NA	94.02	91.43	NA	NA	NA	89.13 ±6.36
3.00×10^{-5}	83.48	NA	97.22	92.61	NA	NA	NA	91.10 ±7.00

Supplementary Table 4. Inhibitory effect of **19a** on hERG

Concentration (M)	Inhibitory effect (%)								Mean±SD (%)
	cell 1	cell 2	cell 3	cell 4	cell 5	cell 6	cell 7	cell 8	
1.00×10^{-9}	NA	NA	NA	NA	NA	-0.91	-0.91	-0.10	-0.64 ±0.47
3.00×10^{-9}	NA	NA	NA	NA	NA	-5.48	-5.48	0.75	-3.40 ±3.60
3.00×10^{-7}	79.02	69.69	75.87	NA	NA	NA	NA	NA	74.86 ±4.75
1.00×10^{-6}	86.59	78.52	81.12	NA	NA	NA	NA	NA	82.08 ±4.12
3.00×10^{-6}	87.46	NA	NA	88.50	94.17	NA	NA	NA	90.04 ±3.61
1.00×10^{-5}	89.18	NA	NA	91.09	97.26	NA	NA	NA	92.51 ±4.23
3.00×10^{-5}	88.58	NA	NA	90.64	96.50	NA	NA	NA	91.91 ±4.10

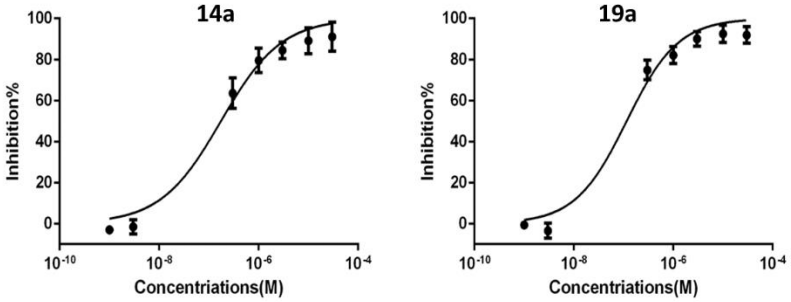

Supplementary Figure 7. Activity of **14a** and **19a** against hERG potassium channel in HEK293 cells. Data points represent ±SD

Supplementary Figure 8. ^{1}H NMR of 9a

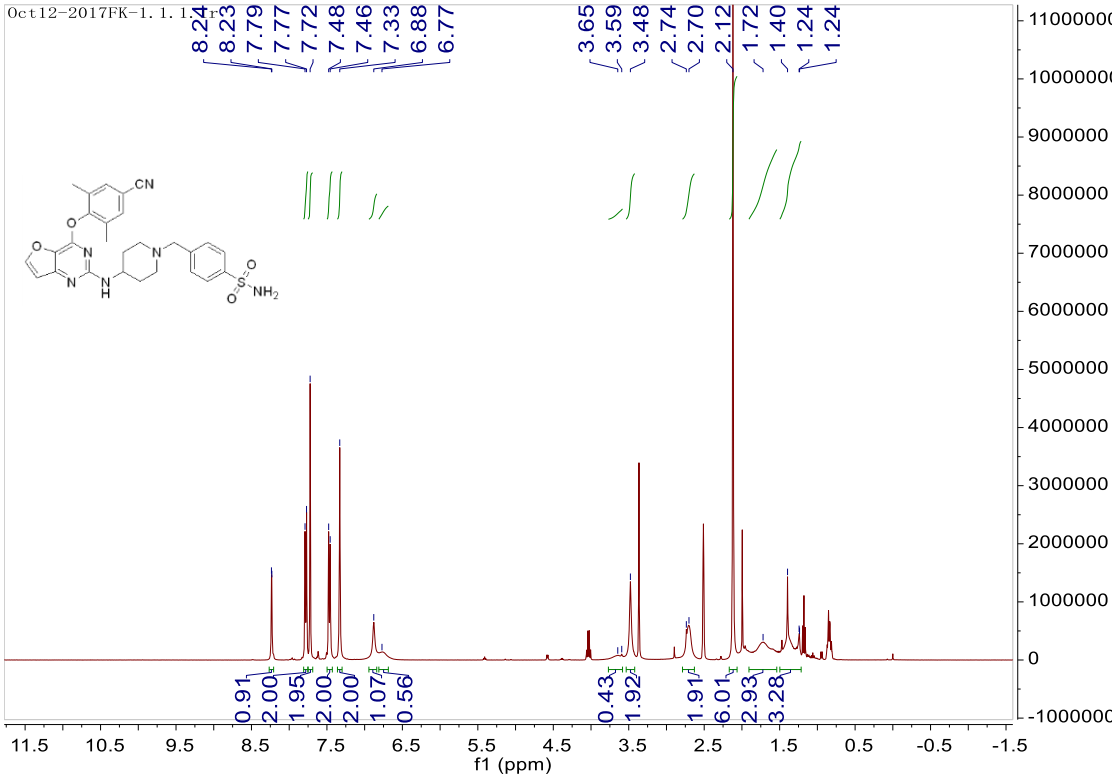

^{13}C NMR of 9a

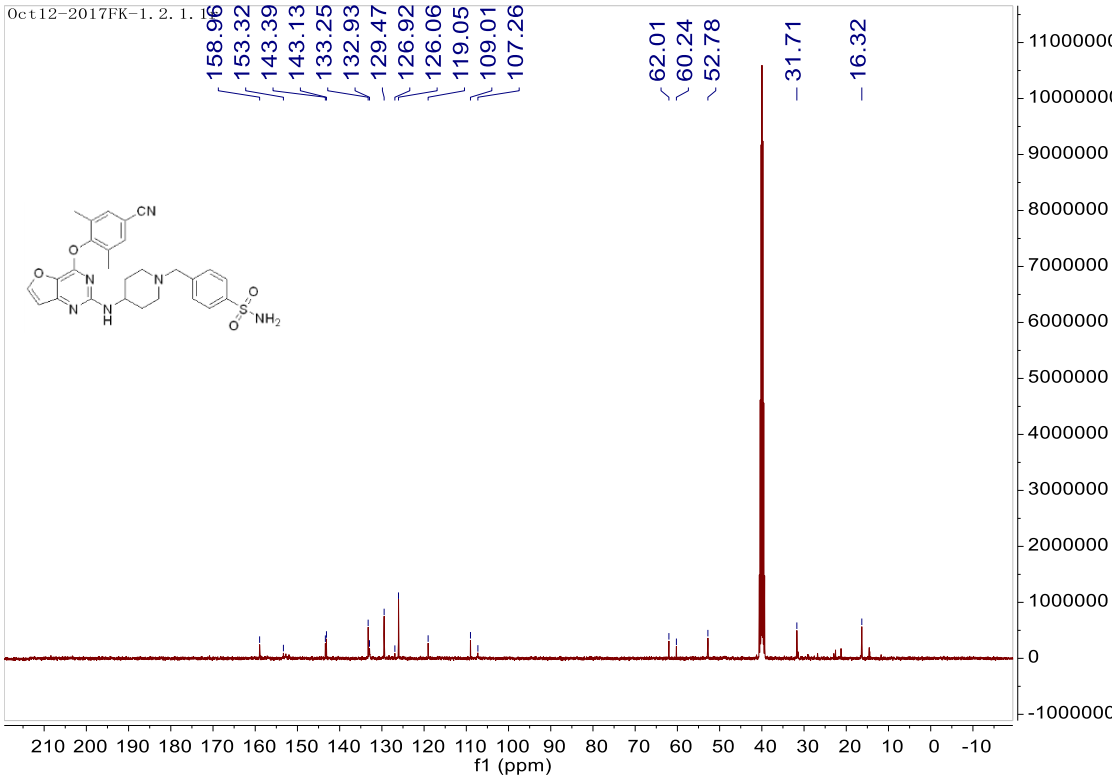

Supplementary Figure 9. ^{1}H NMR of 9b

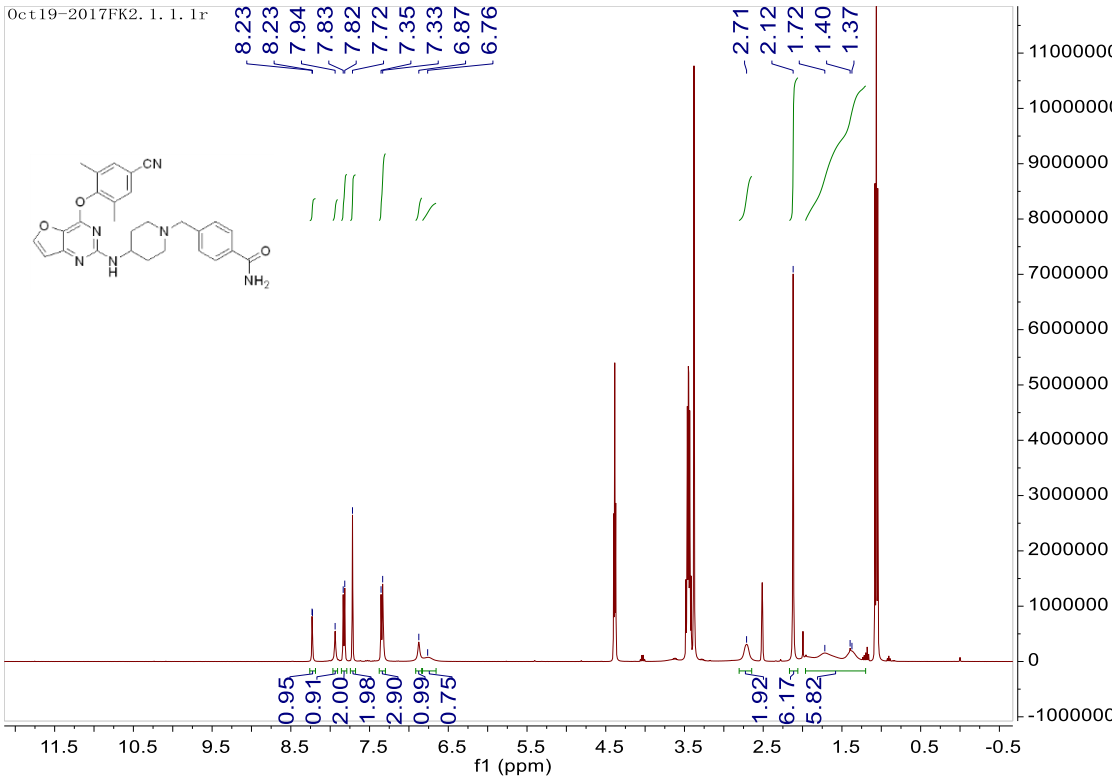

^{13}C NMR of 9b

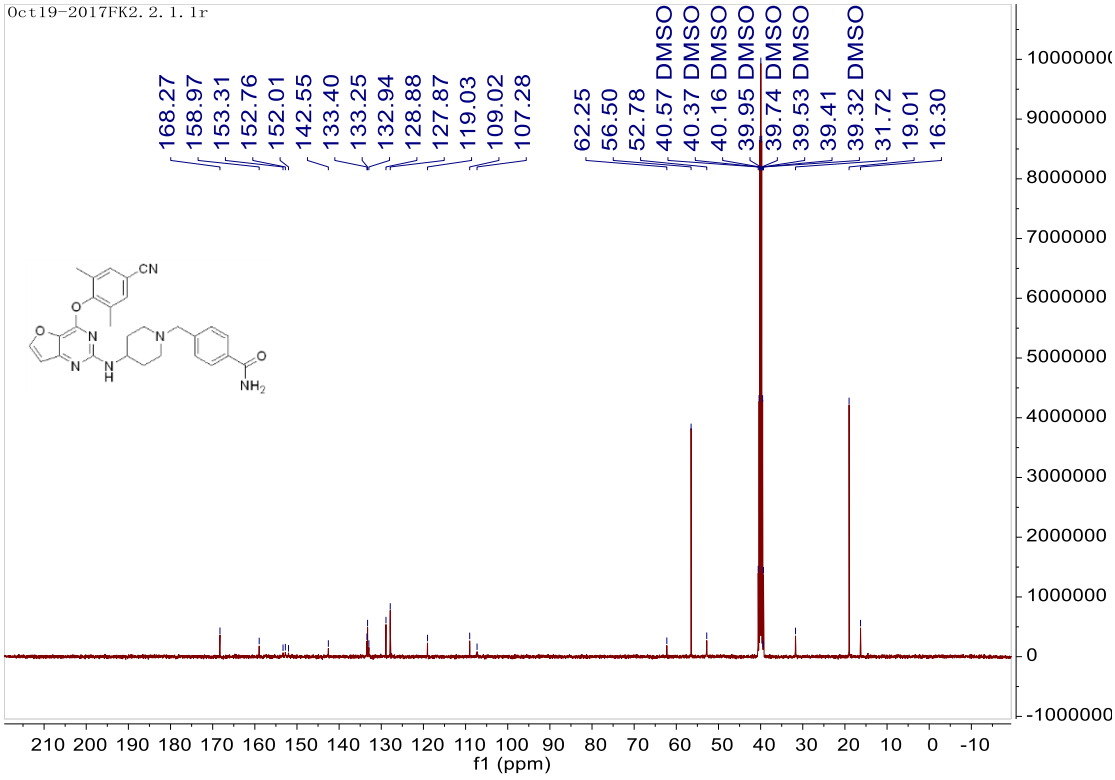

Supplementary Figure 10. ^{1}H NMR of 9c

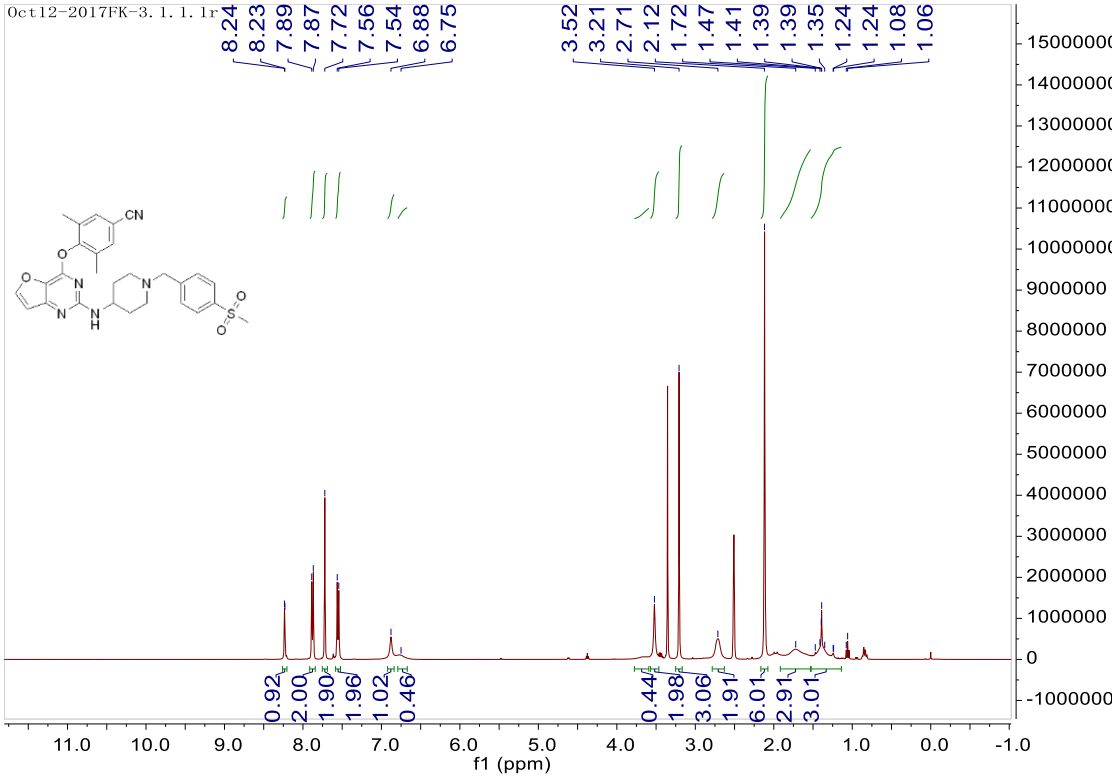

^{13}C NMR of 9c

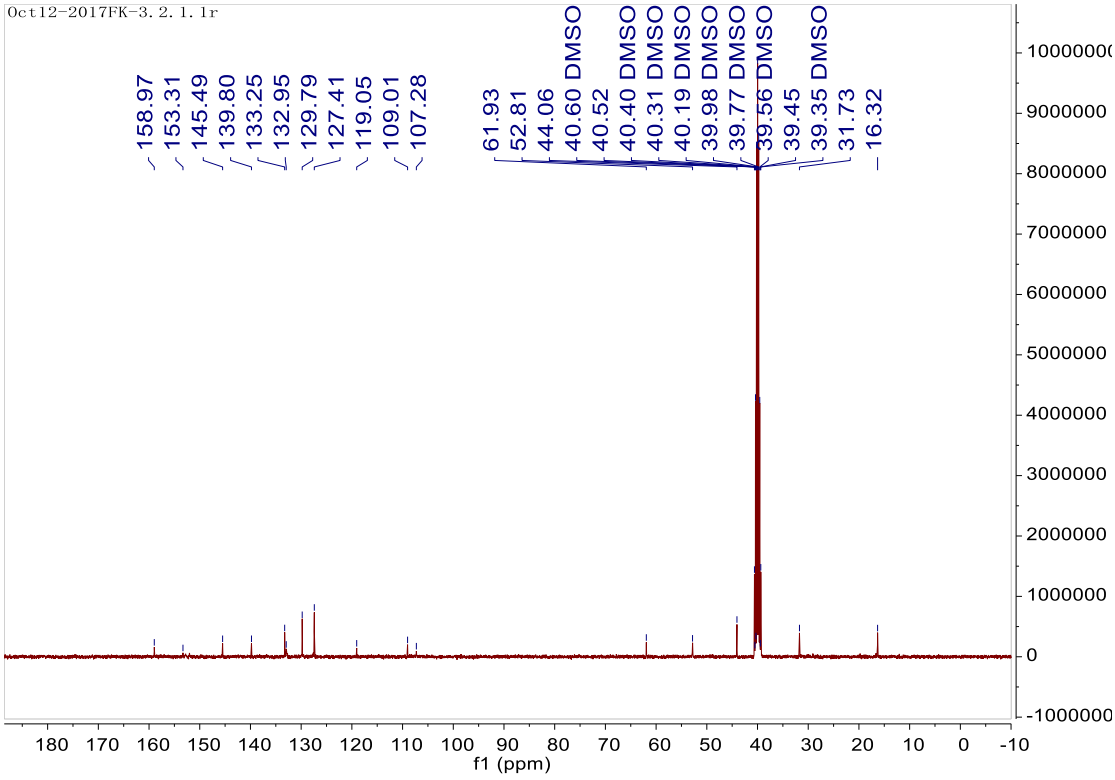

Supplementary Figure 11. ^{1}H NMR of 9d

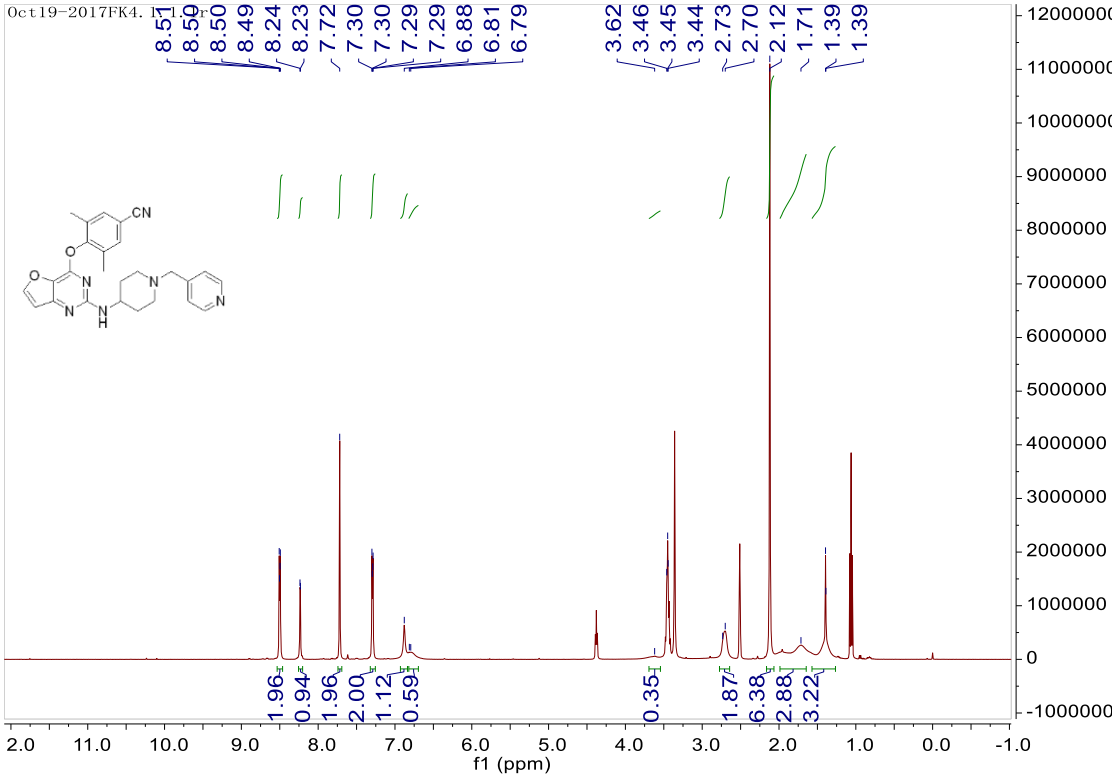

^{13}C NMR of 9d

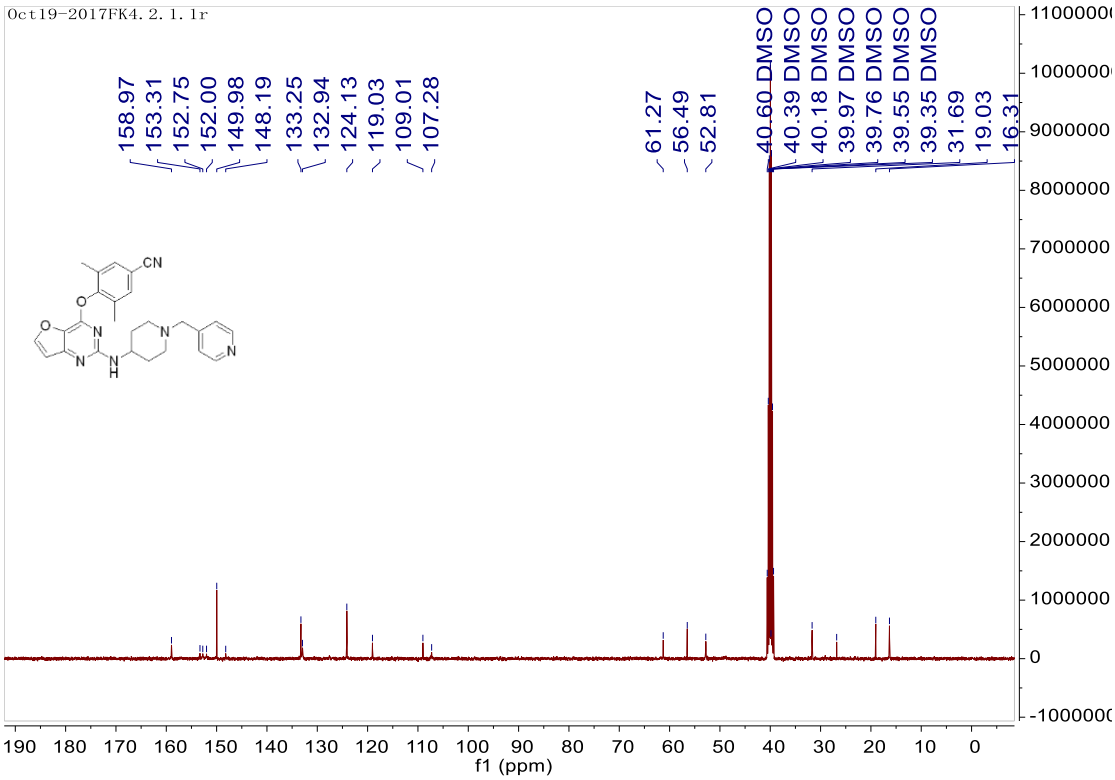

Supplementary Figure 12. ^{1}H NMR of 9e

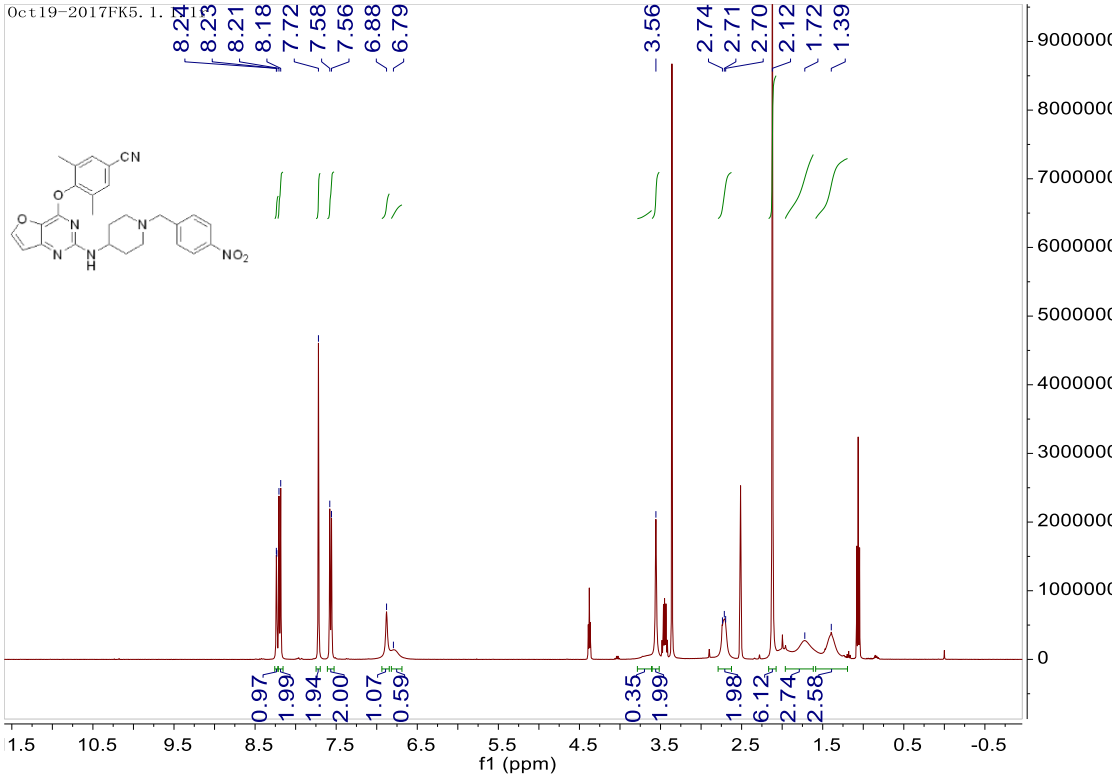

^{13}C NMR of 9e

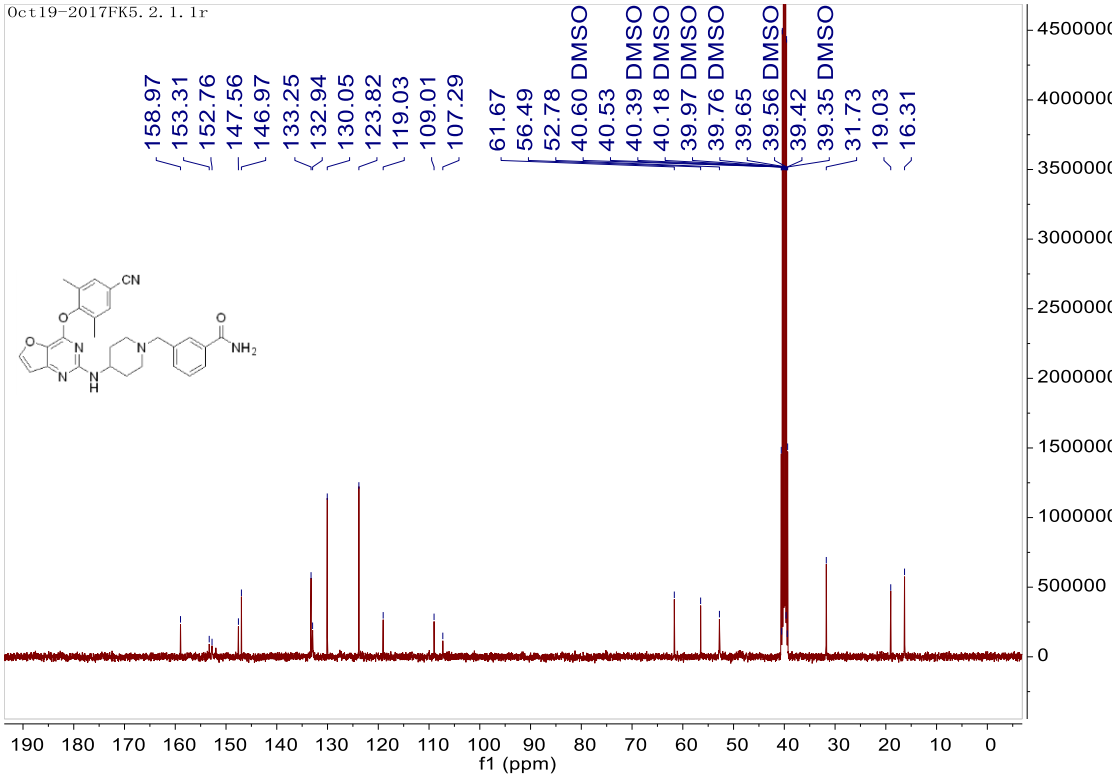

Supplementary Figure 13. ^{1}H NMR of 9f

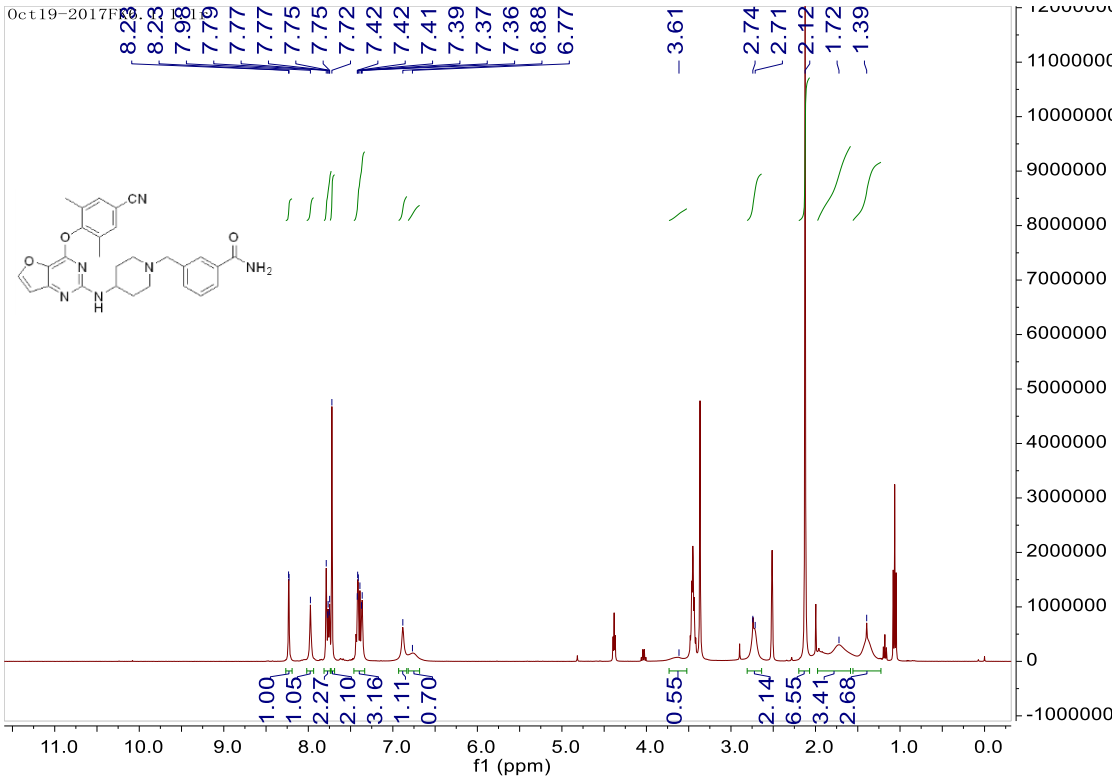

^{13}C NMR of 9f

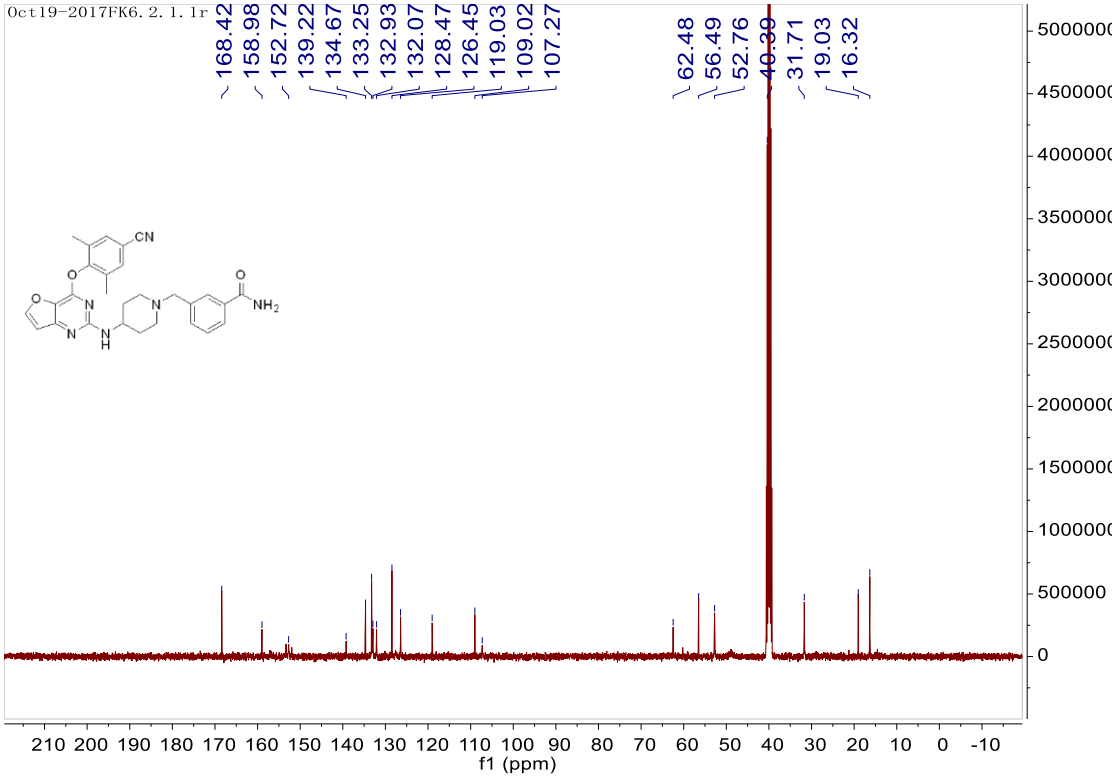

Supplementary Figure 14. ^{1}H NMR of 19a

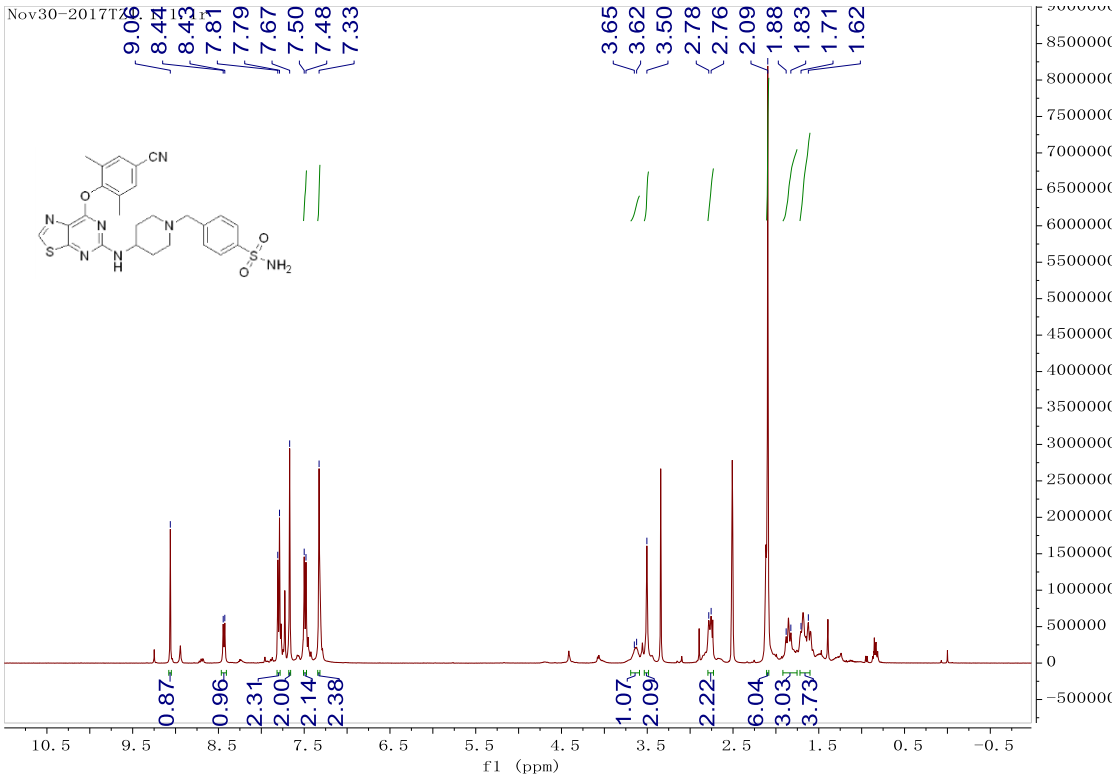

^{13}C NMR of 19a

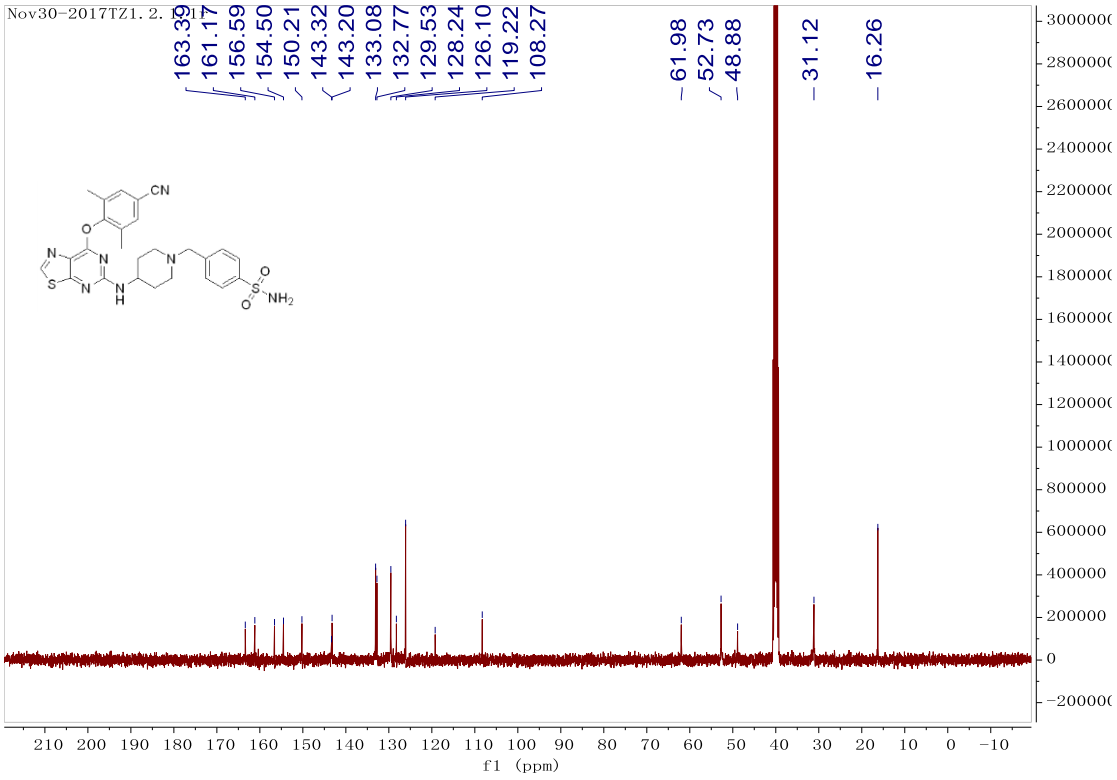

Supplementary Figure 15. ^{1}H NMR of 19b

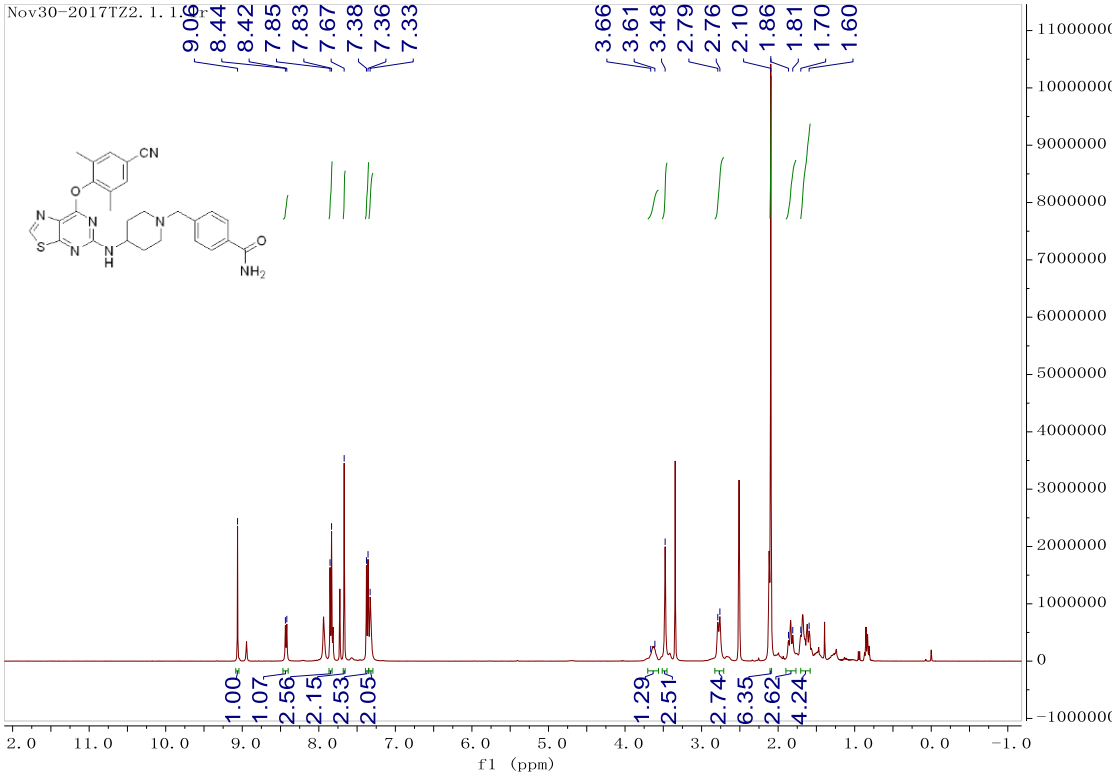

^{13}C NMR of 19b

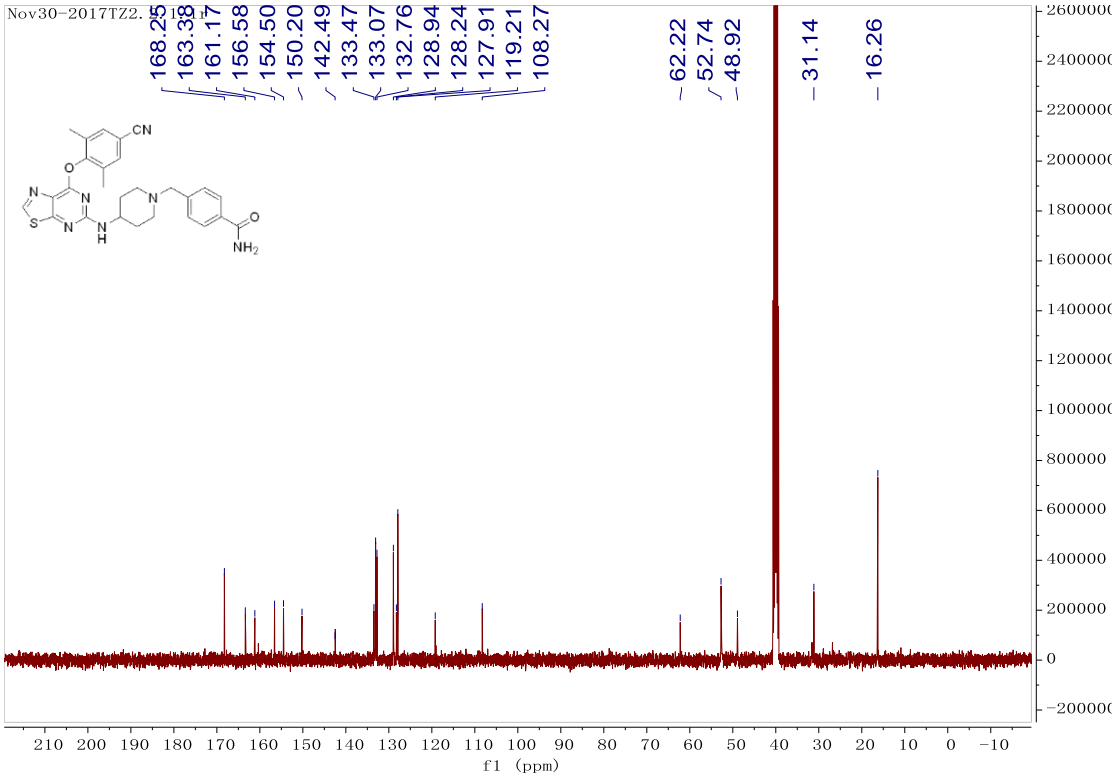

Supplementary Figure 16. ^{1}H NMR of 19e

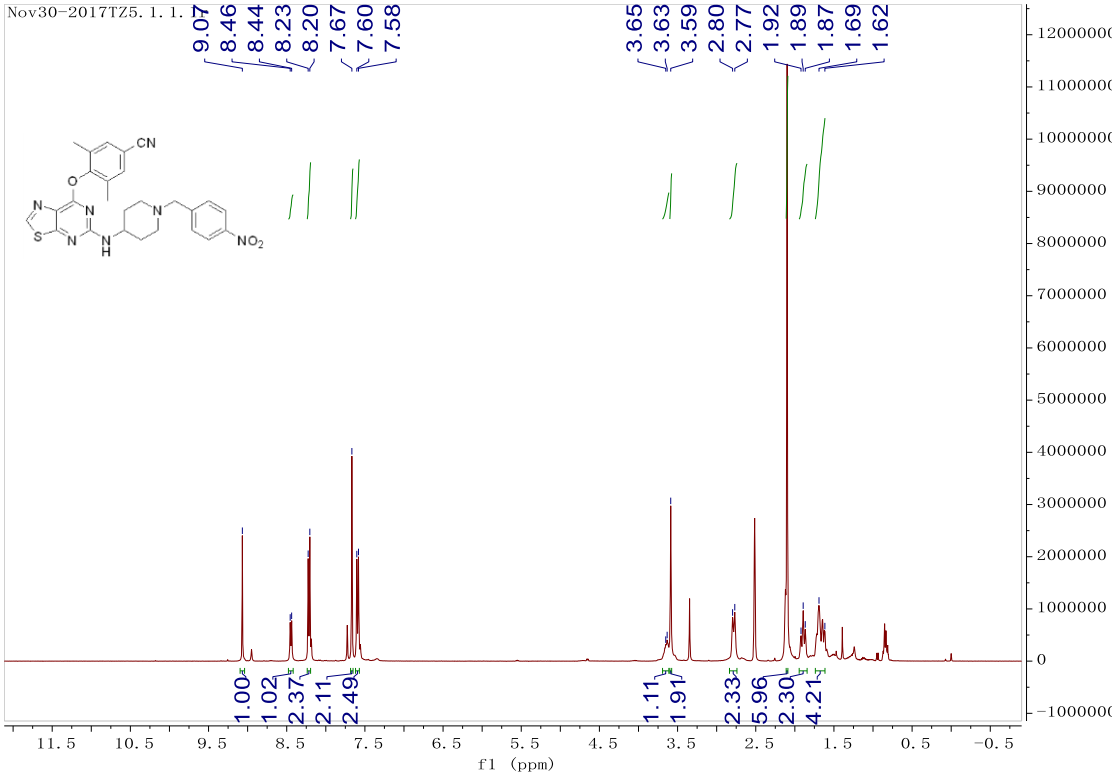

^{13}C NMR of 19e

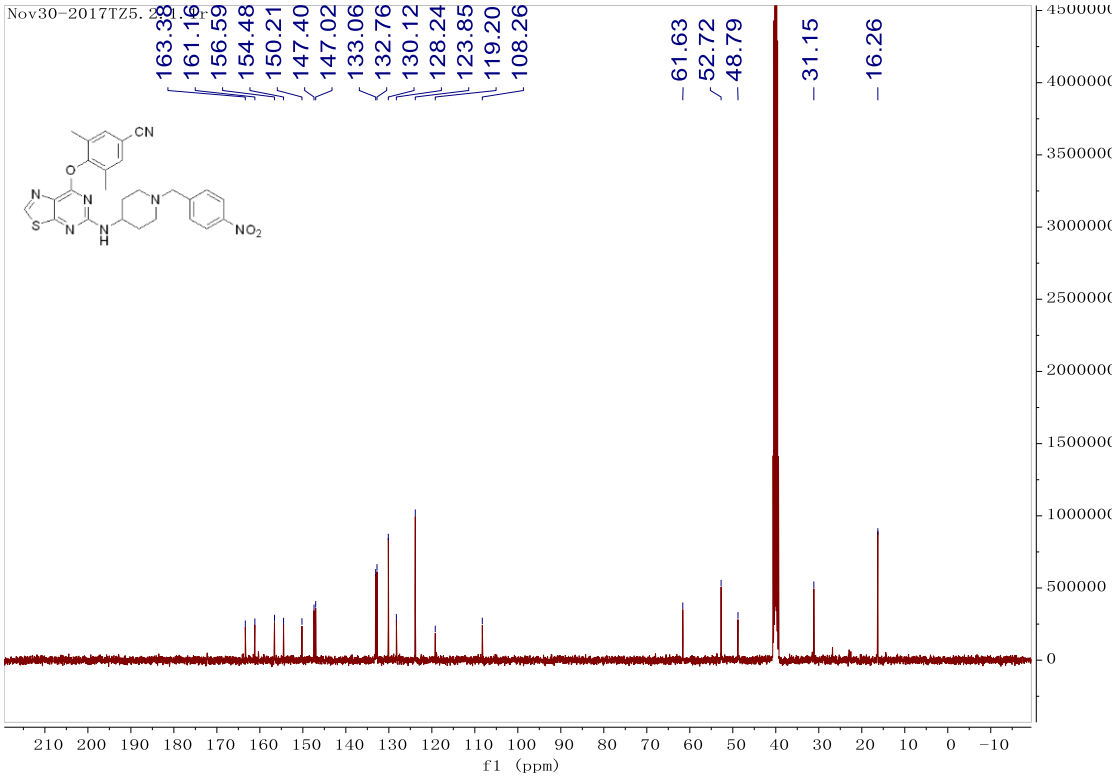

Supplementary References

1. Christophe P, Dirk D, Erik DC. Tetrazolium-based colorimetric assay for the detection of HIV replication inhibitors: revisited 20 years later. *Nature Protocols* **3**, 427-434 (2008).

2. Suzuki K, Craddock BP, Okamoto N, Kano T, Steigbigel RT. Poly A-linked colorimetric microtiter plate assay for HIV reverse transcriptase. *Journal of Virological Methods* **44**, 189 (1993).

3. Yang Y*, et al.* Structural basis for potent and broad inhibition of HIV-1 RT by thiophene[3,2-d]pyrimidine non-nucleoside inhibitors. *eLife* **7**, e36340 (2018).

4. Zhang J*, et al.* Optimization of N-Substituted Oseltamivir Derivatives as Potent Inhibitors of Group-1 and -2 Influenza A Neuraminidases, Including a Drug-Resistant Variant. *Journal of Medicinal Chemistry* **61**, 6379-6397 (2018).

5. LigPrep. Schrödinger, LLC, New York, NY, 2018.

6. Wu G*, et al.* Design, synthesis and biological evaluation of tacrine-1,2,3-triazole derivatives as potent cholinesterase inhibitors. *MedChemComm* **9**, 149-159 (2018).

7. Genheden S, Ryde U. The MM/PBSA and MM/GBSA methods to estimate ligand-binding affinities. *Expert Opinion on Drug Discovery* **10**, 449-461 (2015).

8. Greenidge PA, Kramer C, Mozziconacci JC, Wolf RM. MM/GBSA binding energy prediction on the PDBbind data set: successes, failures, and directions for further improvement. *Journal of Chemical Information and Modeling* **53**, 201-209 (2013).

9. Chen X, Zhan P, Li D, De Clercq E, Liu X. Recent advances in DAPYs and related analogues as HIV-1 NNRTIs. *Current Medicinal Chemistry* **18**, 359-376 (2011).

10. Katchman AN, John K, Toshimasa T, Woosley RL, Ebert SN. Comparative evaluation of HERG currents and QT intervals following challenge with suspected torsadogenic and nontorsadogenic drugs. *Journal of Pharmacology & Experimental Therapeutics* **316**, 1098-1106 (2006).